Received: 21 June 2024 | Revised: 9 December 2024 | Accepted: 15 December 2024

DOI: 10.1002/jex2.70029

RESEARCH ARTICLE

Establishment of an experimental system to analyse extracellular vesicles during apoplastic fungal pathogenesis

Nathaniel Hearfield[1] | **Dominik Brotherton**[2] | **Zedi Gao**[2] | **Jameel Inal**[2,3] | **Henrik U. Stotz**[1,2]

[1]Centre for Agriculture, Food and Environmental Management, University of Hertfordshire, Hatfield, UK

[2]School of Life & Medical Sciences, University of Hertfordshire, Hatfield, UK

[3]School of Human Sciences, London Metropolitan University, London, UK

Correspondence
Henrik U. Stotz, Centre for Agriculture, Food and Environmental Management, University of Hertfordshire, Hatfield, UK.
Email: h.stotz@herts.ac.uk

Funding information
Biotechnology and Biological Sciences Research Council, Grant/Award Number: BB/R019819/1; British Society for Plant Pathology

Abstract

Phoma stem canker disease of oilseed rape (*Brassica napus*) is caused by the extracellular fungal pathogen *Leptosphaeria maculans*. Although this pathogen resides exclusively in apoplastic spaces surrounding plant cells, the significance of extracellular vesicles (EVs) has not been assessed. Here, we show a method to collect apoplastic fluids (AFs) from infected leaves or cotyledons for collection of EVs during the process of host colonisation. The 15,000 × *g* supernatants of AFs were shown to contain ribulose-bisphosphate carboxylase (RuBisCO) at 7 days post-inoculation with *L. maculans*, a protein that was absent from unchallenged cotyledons. RuBisCO release coincided with the switch from biotrophy to necrotrophy, suggesting the involvement of host cell death. However, RuBisCO release did not differ between compatible and incompatible interactions, suggesting necrotrophic host cell death might not be the only process involved. EVs were also collected from axenic fungal cultures and characterised for their particle size distribution using nanoparticle tracking analysis and transmission electron microscopy. The protein composition of EV-enriched fractions was analysed using SDS-PAGE and proteomics. Enrichment analysis of gene ontology terms provided evidence for involvement of glucan and chitin metabolism as well as catalase and peptidase activities. Most of the proteins identified have previously been found in EV studies and/or EV databases, and for most of the proteins evidence was found for an involvement in pathogenicity/virulence.

KEYWORDS
apoplast, extracellular vesicles, nanoscale, pectin, phytopathogen, protein network

1 | INTRODUCTION

Oilseed rape (*Brassica napus*) is the most important temperate oilseed crop, accounting for 86 million metric tonnes in 2021 with major cultivation areas in Europe, Canada, China, Australia and India (FAO). A major disease of worldwide importance is phoma stem canker (Zheng et al., 2020), caused by two related *Leptosphaeria* species, of which *Leptosphaeria maculans* is the more aggressive facilitated via a multitude of effectors (Jiquel et al., 2022). This pathogen causes up to 37% yield loss on average and an estimated 1.6 bn USD in global losses (Cai, Huang et al., 2018). Control of the disease currently involves varying sowing times to avoid infection during early crop growth, using a 4-year interval between oilseed rape crops, sowing fields 50–500 m apart from each other to avoid the spread of ascospores, breeding resistant cultivars of *B. napus*, and fungicide treatments (Hwang et al., 2016). However, these methods only provide limited protection from *L. maculans* as new genetic variants can overcome environmental factors and genetic resistance through effector evolution. More research is necessary to identify novel disease

markers and to better understand the pathogen-host interaction, with the goal of developing sustainable treatments to reduce yield losses.

Although *L. maculans* is an apoplastic fungal pathogen (Stotz et al., 2014), the role of extracellular vesicles (EVs) has not been explored. In contrast, EVs have been shown to influence interactions between plants and biotrophic (An et al., 2006) or necrotrophic pathogens (Cai, Qiao et al., 2018). Plants, including *Arabidopsis thaliana*, produce different types of EVs that can be collected from apoplastic fluids (AFs). Tetraspanin (TET)-positive EVs, representing exosomes derived from multivesicular bodies (MVBs), remain in the supernatant at 40,000 × *g* but pellet at 100,000 × *g* (Cai, Qiao et al., 2018). PEN1-positive EVs, containing a membrane-associated syntaxin involved in penetration resistance against powdery mildew (Collins et al., 2003), pellet at 40,000 × *g* (Rutter & Innes, 2017). Other EVs include exocyst-positive organelle (EXPO)-derived EVs that are larger than exosomes with a diameter of 200–500 nm (Cai et al., 2023). EV functions vary depending on their cargoes, including metabolites (Jeon et al., 2023), lipids, proteins and a variety of nucleic acids (Stotz et al., 2022).

EVs from a limited set of ascomycete plant pathogens have been analysed. Scientific reports include *Zymoseptoria tritici*, which, like *L. maculans*, has an apoplastic lifestyle (Stotz et al., 2014). EVs collected from culture filtrates of *Z. tritici* at 100,000 × *g* contained a smaller percentage of carbohydrate-active enzymes, proteases, effectors and signal peptide-containing proteins than soluble proteins from the supernatant (Hill & Solomon, 2020). Conversely, a larger percentage of proteins with transmembrane domains and GPI-anchors was observed in the EV fraction than amongst the soluble proteins. The cotton pathogen *Fusarium oxysporum* f. sp. *vasinfectum* and the corn pathogen *Fusarium graminearum* produce EVs that contain a purple phytotoxin and putative virulence effectors, respectively (Bleackley et al., 2020; Garcia-Ceron et al., 2021). *Penicillium digitatum* produces EVs containing phytotoxins and mycotoxins in vitro and during citrus fruit infection (Costa et al., 2021). *Colletotrichum higginsianum* produces EVs that contain biosynthetic proteins involved in production of higginsianin A to E, including the phytoactive higginsianin B (Rutter et al., 2022). *C. higginsianum* EVs also contain proteins involved in biosynthesis of a lavostatin-like compound potentially contributing to Dothidiomycete pathogenicity.

The ultimate challenge is to collect pathogen and host EV populations during infection. Fluorescent tags have been developed to differentiate TET-positive and PEN1-positive EVs in *A. thaliana* (He et al., 2021). Similar approaches are being used to tag and trace fungal EVs (Rutter et al., 2022). A combination of fungal and host tags could be used to differentiate host and pathogen EVs during infection. Apoplastic fungal pathogens, like *L. maculans*, may offer advantages because both pathogen and host EVs could be isolated from AFs during infection.

Here we demonstrate the first steps in establishing the interaction between *L. maculans* and *B. napus* as a tool for interkingdom EV research. This pathosystem offers advantages because compatible and incompatible interactions can be readily differentiated. The *R* gene-mediated resistance we have exploited is based on the recognition of the *AvrLm1* effector by the corresponding *LepR3*-encoded receptor (Larkan et al., 2013). During compatible interactions, apoplastic foliar colonisation includes an asymptomatic period of hyphal growth between cells until 5 days post-inoculation (dpi) before the onset of host cell death at 7 dpi (Elliott et al., 2008). This pilot study includes an initial characterisation of AFs from uninfected and infected *B. napus* leaves using nanoparticle tracking analysis (NTA) and sodium dodecyl sulphate-polyacrylamide gel electrophoresis (SDS-PAGE). EVs were collected from culture fluids of *L. maculans* for NTA, transmission electron microscopy (TEM) and proteomic analysis to identify characteristic marker proteins and virulence factors.

2 | MATERIALS AND METHODS

2.1 | Plant and pathogen materials

A. thaliana ecotype Col-0, *B. napus* lines Ningyou1 and Ningyou7 (Source: OCRI, Wuhan, China), and introgression line Topas-*LepR3* in the background of doubled-haploid Topas DH 16516 (Source: Agriculture and Agri-Food Canada, Saskatoon, SK) were used (Larkan et al., 2016). *L. maculans* isolates v23.11.9 (*AvrLm1*, *avrLm2*, *avrLm4-AvrLm7*, *AvrLm5*, *AvrLm6*, *AvrLm8*) and v23.2.1 (*avrLm1*, *avrLm2*, *AvrLm4-AvrLm7*, *AvrLm5*, *AvrLm6*, *AvrLm8*) were obtained from INRA Thiverval-Grignon, France (Balesdent et al., 2001; Rouxel et al., 2003).

2.2 | Plant and pathogen growth

B. napus seeds were pre-germinated on filter paper (20 seeds)R for 2 days before transplanting them into pots containing John Innes Compost No. 3 and Miracle-Gro compost (1:1). Seedlings were grown in controlled environment cabinets (Fitoclima 1200; Aralab, Rio de Mouro, Portugal) at 20°C with a photoperiod of 12 h light/12 h dark, a light intensity of 300 μmol m^{-2} s^{-1} and 60% relative humidity. *A. thaliana* ecotype Col-0 seedlings were grown in soil under the same conditions for 3–4 weeks to harvest leaves at the rosette stage.

Conidial suspensions were prepared from sporulating cultures on V8 agar or potato dextrose agar (Stotz et al., 2023). Conidial suspensions (400 µL) of *L. maculans* strains v23.11.9 (10^8 mL^{-1}) and v23.2.1 (10^6 mL^{-1}) were used to inoculate 400 mL Gamborg B5 medium including vitamins (Duchefa Biochemie, RV Haarlem, Netherlands) containing sucrose (30 g L^{-1}) in 10 mM 2-(*N*-morpholino) ethanesulfonic acid (MES), pH 6.8. Fungal cultures were grown using a MaxQ 800 orbital shaker (Thermo Fisher Scientific Inc., MA, USA) at 130 rpm for 2 weeks at 26°C. A mock-inoculated culture medium control was used to eliminate false positive data.

2.3 | Pathogen inoculation

B. napus seedlings were grown for 10 days and 21 days after germination for inoculation with *L. maculans* at cotyledon and true leaf stages, respectively. Cotyledons and leaves were inoculated using standard protocols (Huang et al., 2003). A sterile pin was used to puncture the adaxial leaf surface twice or four times depending on leaf area without penetrating through to the abaxial side. Wound sites on the leaf were inoculated with 10 µL conidial suspensions (10^6 mL^{-1}). Mock inoculations with sterile water were used as controls. Potted plants were placed in trays with lids to maintain high humidity for 48 h. For this purpose, leaves and lids were sprayed with a fine mist of sterile deionised water, following inoculation.

2.4 | Collection and partial purification of apoplastic fluids

AFs were collected from inoculated true leaves at 4 dpi or cotyledons at 7 dpi. Detached leaves were rinsed with distilled water to remove surface contaminants and blotted dry using paper towels. Leaves or cotyledons were fitted into 60 mL syringes containing a recommended (Cai, Qiao et al., 2018; Rutter & Innes, 2017) infiltration buffer (20 mM MES, 0.1 M NaCl, 2 mM $CaCl_2$, pH 6). Vacuum was applied by covering the syringe opening and pulling the plunger by hand until leaves/cotyledons darkened. Leaves or cotyledons were then rolled within Parafilm strips and inserted into 20 mL syringes so that cut edges were facing the top of the syringe. These were then placed within 50 mL Falcon tubes (Corning, NY, USA) and centrifuged at 4°C and 700 × *g* for 20 min or 1000 × *g* for 10 min until the dark patches of infiltration buffer were removed from the leaves. Collected AFs were transferred to 1.5 mL tubes.

AFs were processed using different centrifugation protocols. Supernatants were analysed after centrifugation at 3000 × *g* and 4°C for 15 min. Alternatively, AFs from inoculated leaves or cotyledons were centrifuged at 15,000 g and 4°C for 15 min prior to analysis of supernatants. In agreement with a recent critical assessment, the isolation procedures reported above are expected to yield plant EVs (Pinedo et al., 2021).

2.5 | Collection and fractionation of extracellular vesicles from fungal cultures

Fluids from liquid fungal cultures were filtered through sterile Miracloth (Merck Millipore, Watford, UK). Fractionation of filtrates followed published procedures with modifications (Reis et al., 2019). Filtrates were centrifuged at 5000 × *g* for 15 min at 4°C. Supernatants were passed through 0.45 µm syringe filters and centrifuged at 15,000 × *g* for 15 min at 4°C to remove debris. Supernatants were spun again at 100,000 × *g* for 1 h at 4°C using a Sorvall™ WX+ ultracentrifuge with an AH-650 swinging bucket rotor (Thermo Fisher Scientific Inc., MA, USA). Supernatants were discarded and pellets were rinsed with phosphate-buffered saline (PBS) before resuspension in 1 mL of PBS. These EV-enriched fractions were separated into 100 µL aliquots, frozen in liquid nitrogen and stored at −80°C. The described protocols adhered to the minimum information for studies of extracellular vesicles (MISEV) as much as possible (Thery et al., 2018; Welsh et al., 2024).

2.6 | Protein quantification, SDS-PAGE and immunoblot analysis

A Bio-Rad DC microplate protein assay (Bio-Rad Laboratories Ltd., Watford, UK) was used for protein quantification using bovine serum albumin (BSA) as a standard. Proteins were separated using discontinuous SDS-PAGE (Laemmli, 1970). A broad-range SDS-PAGE standard (Bio-Rad Laboratories Ltd., Watford, UK) was used to determine molecular weights. Proteins were detected by silver staining (Switzer et al., 1979).

Immunoblot analysis was done after transfer of proteins from the SDS-PAGE gel to polyvinylidene fluoride (PVDF) membrane using a Wet/Tank Blotting System (BioRad). Antibody detection followed standard procedures with 3000-fold dilutions (v/v) of monoclonal mouse anti-ribulose-1,5-bisphosphate carboxylase (RuBisCO) primary antibody (Antibodies.com, Cambridge, UK) and anti-mouse IgG-horseradish peroxidase conjugate as a secondary antibody after blocking with Tween 80. Chemiluminescent

assay followed standard procedures using enhanced chemiluminescence (ECL) reagents (Thermo Fisher Scientific Inc., MA, USA) and a myECL imager (Thermo Fisher Scientific Inc., MA, USA) for detection.

2.7 | Nanoparticle tracking analysis

Samples collected from uninoculated leaf apoplasts or fungal culture medium were analysed by NTA using a NanoSight LM10 (Malvern Instruments), with a green, 532 nm laser module. Software used was NanoSight NTA v2.3 located at the University of Hertfordshire School of Physics, Engineering and Computer Science material laboratory to estimate particle size based on relative movement due to Brownian motion. Samples were diluted to 1:10, 1:100, or 1:1000 and compared to phosphate-buffered saline (PBS) controls. NTA measurements were taken in static mode with three replicates, using a detection threshold = 5 with software version 3.2 Dev Build 3.2.16.

2.8 | Transmission electron microscopy

TEM followed recommended procedures (Gallagher et al., 2019). Formvar-carbon-coated 300 mesh copper grids (Electron Microscopy Science) were first exposed to 1% (w/v) Alcian Blue (Sigma Aldrich). Samples of the EV-enriched fractions were then applied to grids, followed by negative staining using 2% (w/v) phosphotungstic acid. Sample-containing grids were air-dried before analysis using TEM; images were accessed using a JEM-1400Flash electron microscope (JEOL) at the Duncan Calder Materials Microscopy Laboratory of the University of Hertfordshire.

2.9 | Proteomics

Protein samples of the EV preparations of isolates v23.2.1 and v23.11.9 were briefly separated using SDS-PAGE. Shortly after entering the separating gel, staining with Coomassie Brilliant blue R-250 was used to visualise protein bands that were then excised. The gel slice of isolate v23.11.9 was sent to the Cambridge Centre for Proteomics for analysis. A tryptic digest was done and identified peptide sequences were analysed further using the Mascot database.

Cambridge Centre for Proteomics shared an MHT file containing UniProt IDs that were accessed to obtain amino acid sequences. InterProScan was used to identify constituent domains and to determine annotated subcellular localisations of identified proteins.

2.10 | Computational analysis of proteome data

The gene ontology (GO) terms of a subset of 103 proteins identified at the Cambridge Centre for Proteomics as belonging to *L. maculans* were determined with a focus on the GO category for molecular function (MF). A GO term enrichment analysis was done in R using the published proteome for *L. maculans* isolate JN3 as a reference (Rouxel et al., 2011). Fisher's exact test was used to determine statistical significance.

The subset of 103 *L. maculans* proteins was entered into the STRING database to visualise a protein-protein interaction network (Szklarczyk et al., 2023). The PHI-base 4.16 protein sequences database was used for basic local alignment search tool (BLAST) searches to identify annotated virulence factors (Urban et al., 2022). Sequences of the subset of 103 *L. maculans* proteins were also used to interrogate the EVpedia database (Kim et al., 2015). Text searches were also done using Vesiclepedia, Google Scholar and PubMed Central (Chitti et al., 2024).

3 | RESULTS

3.1 | Release of ribulose-1,5-bisphosphate carboxylase into the apoplast of *B. napus* leaves infected with *L. maculans*

To better understand apoplastic pathogenesis caused by *L. maculans*, AFs were collected from uninfected (Figure 1) and infected plants (Figure 2). Analysis of protein composition using SDS-PAGE showed that AFs were devoid of the major protein from leaves, RuBisCO, which is localised in the chloroplast, suggesting that no cellular disruption occurred during AF collection (Figure 1a). Further analysis of AFs using NTA demonstrated peaks ranging from 67 to 509 nm (Figure 1b–d). To our knowledge,

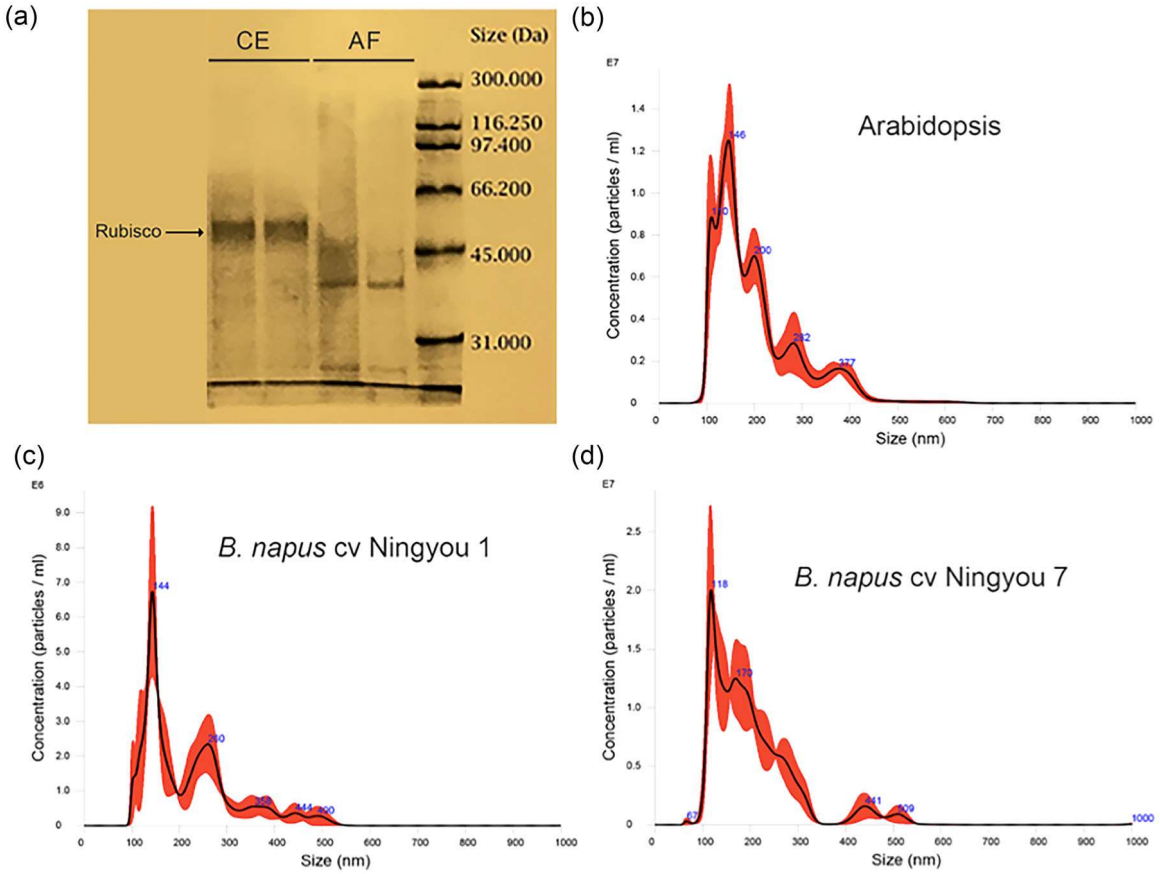

FIGURE 1 Analysis of apoplastic fluids (AFs) from uninfected plants. AFs were collected by centrifugation at 700 × *g*. Following centrifugation at 3000 × *g*, supernatants were used for analyses. (a) SDS-PAGE analysis of proteins from cellular extracts (CE) or AFs from leaves of *Brassica napus*. Samples contained 20 µg protein per lane. Silver staining was used for protein visualisation. Nanoparticle tracking analysis (NTA) of undiluted AFs from leaves of (b) *Arabidopsis thaliana*, (c) *B. napus* cv. Ningyou1 and (d) Ningyou7. Black lines show means of particles of specific sizes (three analytical runs) and red ranges indicate standard errors. Blue numbers provide peaks of particle sizes.

no EVs have been isolated from AFs of *Brassica* leaves. NTA analysis of AF from *B. napus* cv Ningyou 1 (Figure 1c) and Ningyou 7 (Figure 1d) had particle profiles and size distributions like *A. thaliana*, but they apparently contained some larger EVs (>450 nm) than ecotype Col-0 using this experimental system (Figure 1b).

To determine the impact of pathogenesis on the apoplast of *B. napus* leaves, AFs were collected at different stages after *L. maculans* inoculation. Necrotic lesions were observed at 21 days post-inoculation (dpi) of *B. napus* line Topas with either isolate v23.2.1 or v23.11.9 and in Topas-*LepR3* inoculated with v23.2.1 that, unlike v23.11.9, lacks the corresponding effector *AvrLm1* (Figure 2a). Notably, *AvrLm1* seemed to enhance virulence on Topas, suggested by the chlorosis that surrounded the necrotic lesion (Figure 2a). Mock-inoculations with water were used as controls. AFs were collected at 4 dpi from leaves, and proteins were analysed using SDS-PAGE, followed by silver staining or immunoblotting (Figure 2b). Small differences in banding patterns were observed, including more RuBisCO release into the apoplast after inoculation of susceptible Topas with isolate v23.11.9 producing *AvrLm1*. A limited amount of RuBisCO was detected in AFs, even in one of the controls, suggesting that some cellular disruption occurred during collection of AFs for this foliar control sample (Figure 2b). Inoculated samples consistently generated a trace amount of RuBisCO that was detected using immunoblotting. At 7 dpi, stronger bands of RuBisCO were observed in inoculated cotyledons, but mock-inoculated control samples were completely devoid of RuBisCO, suggesting the absence of cellular disruption during collection of AFs (Figure 2c). The amount of RuBisCO from inoculated cotyledons did not vary between compatible (Topas and Topas-*LepR3* inoculated with isolate v23.2.1) or incompatible interactions (Topas-*LepR3* inoculated with isolate v23.11.9). This could either mean that presence of RuBisCO in AFs is independent of the type of interaction or that cell death occurred in response to both compatible and incompatible interactions. In case of compatibility and incompatibility, this might be related to necrosis and programmed cell death, respectively. Another infection-specific band of <31 kDa was observed at this later stage of colonisation. Collectively, these data demonstrate the suitability of using AFs from infected *L. maculans* leaves to better understand the role of EVs during infection with extracellular fungal pathogens.

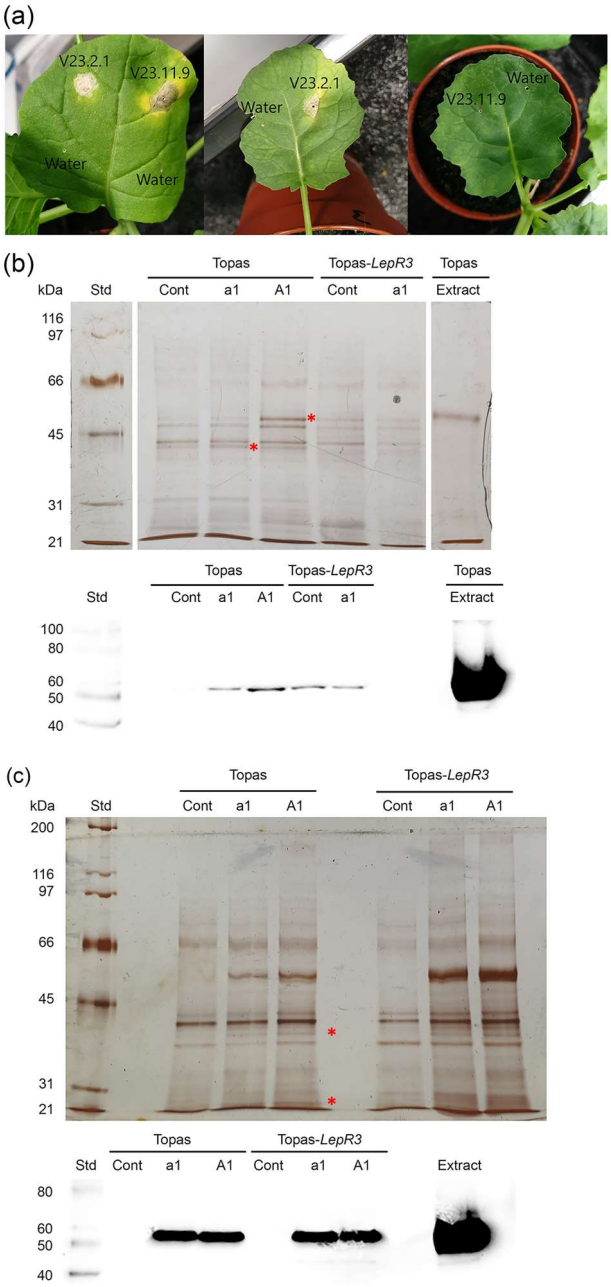

FIGURE 2 Analysis of proteins from apoplastic fluids (AFs) collected after inoculation of *Brassica napus* leaves with *Leptosphaeria maculans*. (a) Compatible and incompatible interactions between *B. napus* and *L. maculans*. Leaves of *B. napus* line Topas DH (left) or Topas-*LepR3* were inoculated with conidial suspensions of isolate v23.2.1 carrying *avrLm1* or v23.11.9 carrying *AvrLm1*. Images were taken 21 days post-inoculation (dpi). Mock inoculations with sterile distilled water were used as a control. SDS-PAGE of AFs collected (b) at 4 dpi from leaves or (c) at 7 dpi from cotyledons of *B. napus* line Topas DH or Topas-*LepR3* inoculated with isolate v23.2.1 (a1) or v23.11.9 (A1). AFs were collected by centrifugation at 1000 × *g* and subsequent centrifugation at 15,000 × *g* before supernatants were analysed by SDS-PAGE. AFs contained 10 μg protein per lane and extracts 2 μg per lane. Silver staining (top) or immunoblotting (bottom) was used for detection. A monoclonal RuBisCO antibody was used for western blotting. Red asterisks indicate protein bands present in infected leaves but not in mock-inoculated controls.

3.2 | Visualisation of EVs from culture fluids of *L. maculans*

To determine whether EVs could be collected from *L. maculans*, conidial suspensions of isolates v23.11.9 and v23.2.1 were used to inoculate Gamborg B5 medium with vitamins. Cultures were maintained for two weeks in an incubator while shaking at 26°C. Fungal colonisation of the medium was readily visible at this stage, culture fluids were collected and EVs fractionated using differential centrifugation at 5000, 15,000 and 100,000 × *g*. The protein concentrations of the resuspended EV pellets at 100,000 × *g* of isolates v23.11.9 and v23.2.1 were 0.52 and 0.20 mg mL^{-1}, respectively, explained by the fact that the primary

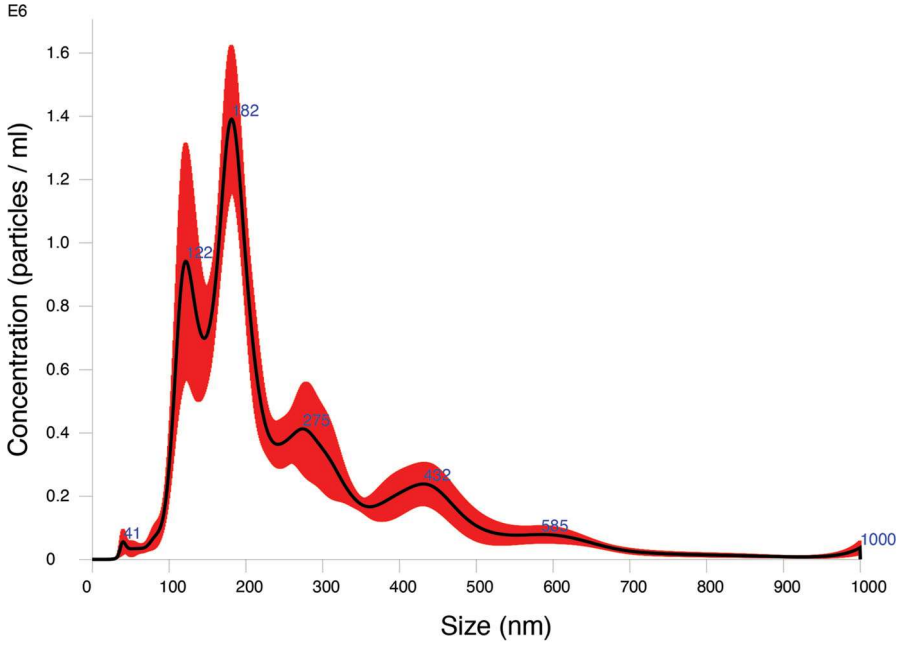

FIGURE 3 Nanoparticle tracking analysis (NTA) of extracellular vesicles (EVs) from culture fluids of *Leptosphaeria maculans* isolate v23.11.9 after growth in Gamborg B5 medium. Differential centrifugation was used to enrich for EVs; the final pellet was collected after centrifugation at 100,000 × *g* and resuspended in PBS. The EV preparation was diluted 1:100, prior to NTA. The size distribution of the particles shown as a black line represents the means of five analytical runs; red ranges illustrate the standard errors. Blue numbers indicate EV particle sizes at specific maxima.

inoculum of isolate v23.11.9 was two orders of magnitude higher than v23.2.1. Liquid growth on potato dextrose broth or V8 broth did not yield satisfactory results.

EV preparations were analysed using NTA. The particle concentrations of isolate v23.11.9 exceeded the particle concentrations of isolate v23.2.1 and both control preparations (Figure S1). The particle concentrations of isolate v23.2.1 were too low to significantly exceed the particle concentrations of the mock-inoculated culture medium control. The PBS control was close to the baseline of detection. The mean particle distribution and error estimates of isolate 23.11.9 were visualised with maxima ranging from 41 to 432 nm (Figure 3).

TEM was used to visualise the EVs from the resuspended 100,000 × *g* pellets of *L. maculans* isolate v23.11.9. Apparent EVs of different sizes were identified (Figure 4), confirming the maxima identified by NTA (Figure 3). Also, relative abundances were confirmed in that larger EVs were rarer than smaller ones. Different types of staining patterns were observed, suggesting the existence of different types of EVs. Some EVs had a cup-shaped morphology.

3.3 | Proteome analysis of EVs from culture fluids of *L. maculans* suggest a role in pathogenesis

The EV fraction isolated from culture filtrates of *L. maculans* isolate v23.11.9 was subjected to proteome analysis. Over 116 proteins were identified using Mascot search parameters, 90% of which had hits to *L. maculans* (Supplementary file 1). Of the 103 *L. maculans* proteins identified, 101 had ≥3 matches to the Mascot database (Table 1). Most of the proteins (60) were annotated by PHI-base to be involved in host interactions, 44 and 16 of which contributed positively and neutrally/negatively to virulence/pathogenicity, respectively. Over half of the proteins (55) delivered matches when searching for sequences using the EVpedia database (Kim et al., 2015). In total, 35 of the predicted proteins lacked a signal peptide with predicted cytosolic (28), nuclear (1) or membrane localisation (6). Most of these proteins (25) had homologs in EVpedia, whereas less than half (30 of 68) of the proteins with predicted signal peptides were found in EVpedia. Most of the proteins lacking signal peptides (24 of 35 or 69%) had pathogenicity annotations, suggesting that non-conventional secretion contributes to virulence of *L. maculans*. Two of the identified proteins, the secreted protein SP1 and necrosis and ethylene-inducing peptide 1 (Nep1), have been characterised in *L. maculans* (Haddadi et al., 2016; Wilson et al., 2002).

SDS-PAGE analysis of EV fractions from isolates v23.2.1 and v23.11.9 demonstrated differences in the distribution of protein bands (Figure 5), which may reflect their different protein concentrations and stages during axenic growth. Although the identities of the major silver-stained bands of isolate v23.11.9 remain elusive, in reference to the proteomics data, candidates may be noted (Table 1).

TABLE 1 *Leptosphaeria maculans* sequence-based proteomics data identified by Mascot searches.

Rank[a]	Protein name[b]	Signal peptide[c]	Theoretical MW[d]	PHI-BLAST annotation[e]	EVpedia hit (E-value)[f]
2	Catalase	Yes	78,998	Bccat2 (*Botrytis cinerea*) unaffected pathogenicity (Schouten et al., 2002)	*Paracoccidioides brasiliensis* (0.0)
5	Similar to glucosyl hydrolase	No	89,890	CDA3 (*Magnaporthe oryzae*) unaffected pathogeneicity (Geoghegan & Gurr, 2016)	*Saccharomyces cerevisiae* (3e-09) (Rizzo et al., 2021)
7	Exo-1,4-beta-D-glucosaminidase	Yes	95,646	bgaA (*Streptococcus pneumoniae*) reduced virulence in mice (Dalia et al., 2010)	No significant hit
8	Similar to exo-beta 1,3 glucanase	No	83,884	No significant hit	No significant hit
9	Glucoamylase	Yes	63,481	SGA1 (*Magnaporthe oryzae*) unaffected pathogenicity (Deng & Naqvi, 2010)	*Trichomonas vaginalis* (7e-07)
10	Beta-hexosaminidase	Yes	65,097	HEX1 (*Candida albicans*) reduced virulence in mice (Ruhela et al., 2015)	Human (6e-57) (Martinez-Lopez et al., 2022)
11	Probable alpha/beta-glucosidase agdC	No	107,584	BcBGL5 (*Botrytis cinerea*) reduced virulence on tomato (Yao et al., 2016)	Human (2e-136)
12	Peptide Hydrolase	Yes	39,461	No significant hit	*Myxococcus xanthus* (9e-47)
13	Similar to subtilisin-like serine protease PR1A	Yes	38,688	Pr1 (*Metarhizium anisopliae*) reduced virulence on *Tenebrio molitor* (Wang et al., 2002)	*P. brasiliensis* (9e-81)
14	Uncharacterized protein	No	76,565	BCIN_03g01540 (*Botrytis cinerea*) reduced virulence on tomato (Zhang et al., 2020)	No significant hit
15	Cellulase domain-containing protein	No	72,033	GLU1 (*Pyrenophora tritici-repentis*) reduced virulence on wheat (Fu et al., 2013)	*P. brasiliensis* (3e-113)
16	Similar to glucan 1,3-beta-glucosidase	Yes	31,628	BcEG (Bcin09g00200) *Botrytis cinerea* reduced virulence on apple (Li et al., 2020)	*S. cerevisiae* (1e-20)
17	Amine oxidase	Yes	51,025	MrMao-1 (MAA_03753) *Metarhizium robertsii* increased virulence (hypervirulence) (Tong et al., 2020)	Mouse (1e-75)
18	Extracellular metalloproteinase MEP	Yes	67,232	Cgfl (GLRG_06543) *Colletotrichum graminicola* effector on maize (Sanz-Martin et al., 2016)	*M. xanthus* (4e-87)
19	Similar to alpha-1,3-glucanase	Yes	49,062	No significant hit	No significant hit
20	Chitin binding protein	Yes	48,675	CDA2 (*Magnaporthe oryzae*) unaffected pathogenicity (Geoghegan & Gurr, 2016)	*S. cerevisiae* (1e-16) (Rizzo et al., 2021)
21	Chitinase	No	43,434	CHT42 (*Trichoderma virens*) reduced virulence against *Rhizoctonia solani* (Baek et al., 1999)	*M. xanthus* (6e-49) (Rutter & Innes, 2023)
22	Similar to glyoxal oxidase	Yes	67,248	GLO1 (*Ustilago maydis*) loss of pathogenicity on maize (Leuthner et al., 2005)	*M. xanthus* (8e-05) (Rizzo et al., 2021)
23	Uncharacterized protein	Yes	80,900	No significant hit	No significant hit
25	Similar to polygalacturonase 1	Yes	37,216	Aapg1 (*Alternaria alternata*) unaffected pathogenicity on *Citrus jambhiri* (Isshiki et al., 2001)	No significant hit

(Continues)

TABLE 1 (Continued)

Rank[a]	Protein name[b]	Signal peptide[c]	Theoretical MW[d]	PHI-BLAST annotation[e]	EVpedia hit (E-value)[f]
26	Non-reducing end alpha-L-arabinofuranosidase	Yes	37,052	No significant hit	No significant hit
27	Pectate lyase	Yes	32,776	PELB (*Colletotrichum gloeosporioides*) reduced virulence on avocado (Miyara et al., 2008)	No significant hit
28	Peptide hydrolase	Yes	50,330	No significant hit	*Pseudomonas aeruginosa* (4e-64)
29	Metallopeptidase	Yes	32,132	No significant hit	
30	alpha-1,2-mannosidase	Yes	54,944	msdS/msdC (*Aspergillus fumigatus*) unaffected pathogenicity in mice (Li et al., 2008)	Human (4e-62)
31	Uncharacterized protein	No	63,639	Ape4 (*Cryptococcus neoformans*) reduced virulence in mice (Gontijo et al., 2017)	Bovine (2e-152)
33	Similar to trypsin-like protease 1	Yes	24,460	GIP1 (*Phytophthora sojae*) effector on soybean (Rose et al., 2002)	Mouse (5e-54)
34	Unknown protein	Yes	74,156	No significant hit	No significant hit
35	Predicted protein	No	61,800	No significant hit	(de Paula et al., 2019)
37	Similar to carboxypeptidase A	Yes	49,967	No significant hit	Human (2e-14)
38	Similar to tripeptidyl-peptidase	Yes	64,292	FGSG_10343 (*Fusarium graminearum*) unaffected pathogenicity on wheat (Lowe et al., 2015)	Human (2e-82)
39	1-alkyl-2-acetylglycero-phosphocholine esterase	Yes	41,711	No significant hit	No significant hit
40	Alpha-amylase	Yes	64,234	SGA1 (*Magnoporthe oryzae*) unaffected pathogenicity on rice and barley (Deng & Naqvi, 2010)	*M. xanthus* (6e-42)
42	Uncharacterized protein	Yes	64,809	BcBGL6 (*Botrytis cinerea*) reduced virulence on tomato (Zhang et al., 2020)	Bovine (1e-66)
44	Uncharacterized protein	Yes	57,167	No significant hit	No significant hit
45	GH131_N domain-containing protein	Yes	30,193	No significant hit	No significant hit
46	Similar to endo-1,3(4)-beta-glucanase	Yes	34,039	Eng1 (*Histoplasma capsulatum*) reduced virulence (Garfoot et al., 2017)	(Vargas et al., 2015)
47	Carboxylic ester hydrolase	Yes	57,360	VTL1 (*Magnaporthe oryzae*) unaffected pathogenicity on rice (Wang et al., 2007)	Bovine (4e-43)
48	Cupin type-1 domain-containing protein	Yes	28,953	FoCupin1 (*Fusarium oxysporum*) effector (Yan et al., 2022)	No significant hit
49	Chitinase	Yes	49,793	CHT42 virulence factor of *Trichoderma virens* against *Rhizoctonia solani* (Baek et al., 1999)	*M. xanthus* (4e-32)
50	Alkaline phosphatase	Yes	73,001	No significant hit	Human (6e-33)

(Continues)

TABLE 1 (Continued)

Rank[a]	Protein name[b]	Signal peptide[c]	Theoretical MW[d]	PHI-BLAST annotation[e]	EVpedia hit (E-value)[f]
51	Probable Xaa-Pro aminopeptidase P	No	67,950	pepP (*Camylobacter jejuni*) reduced virulence in mice (Heimesaat et al., 2020)	*P. brasiliensis* (0.0) (Souza et al., 2019)
52	Similar to endonuclease/exo-nuclease/phosphatase family protein	Yes	63,780	spnA (*Streptococcus pyogenes*) reduced virulence (Chang et al., 2011)	No significant hit
53	Similar to chitin binding protein	Yes	52,786	Cda2 (*Magnaporthe oryzae*) unaffected pathogenicity (Geoghegan & Gurr, 2016)	*S. cerevisiae* (1e-09) (Rizzo et al., 2021)
54	Similar to siderophore esterase IroE-like	No	34,440	IroE (*Escherichia coli*) reduced virulence (Lin et al., 2005)	*M. xanthus* (5e-05)
55	Uncharacterized protein	No	67,358	MoGls2 (*Magnaporthe oryzae*) reduced virulence (Deng et al., 2019)	Human (4e-29)
56	Similar to FAD/FMN-containing isoamyl alcohol oxidase MreA	Yes	66,465	ZEB1 (*Fusarium graminearum*) unaffected pathogenicity (Lysoe et al., 2006)	(Souza et al., 2019)
57	Uncharacterized protein	Yes	13,395	SP1 (*Leptosphaeria maculans*) unaffected pathogenicity (Wilson et al., 2002)	No significant hit
58	Similar to glucan 1,3-beta-glucosidase	Yes	31,181	BGL2 (*Candida albicans*) reduced virulence (Sarthy et al., 1997)	*S. cerevisiae* (3e-61) (Dawson et al., 2020)
59	Uncharacterized protein	No	63,175	BcEG (Bcin09g00200) *Botrytis cinerea* reduced virulence on apple (Ma et al., 2022)	*S. cerevisiae* (4e-16) (Garcia-Ceron et al., 2021)
60	Glutamate dehydrogenase	No	48,847	No significant hit	*P. brasiliensis* (0.0) (Bleackley et al., 2019)
62	Similar to FAD-dependent pyridine nucleotide-disulphide oxidoreductase	No	35,185	Trr2 (*Beauveria bassiana*) reduced virulence (Zhang et al., 2016a)	(Bleackley et al., 2019)
63	Uncharacterized protein	Yes	20,721	No significant hit	No significant hit
64	Uncharacterized protein	Yes	65,157	Bcser2 (*Botrytis cinerea*) reduced virulence on Arabidopsis and tomato (Liu et al., 2020b)	*P. brasiliensis* (0.0)
65	Similar to carboxypeptidase A	Yes	45,912	No significant hit	Human (2e-73)
66	Uncharacterized protein	Yes	39,530	FGSG_02549 (*Fusarium graminearum*) virulence factor on wheat (Dufresne et al., 2008)	(Bleackley et al., 2019)
67	Similar to spermidine synthase	No	33,161	Fgspe3 (*Fusarium graminearum*) reduced virulence on maize and wheat (Tang et al., 2021)	*S. cerevisiae* (2e-156)
68	Similar to YesU	Yes	24,154	No significant hit	No significant hit
69	Uncharacterized protein	No	104,548	No significant hit	No significant hit
70	Similar to histidine acid phosphatase	Yes	52,915	No significant hit	No significant hit

(Continues)

TABLE 1 (Continued)

Rank[a]	Protein name[b]	Signal peptide[c]	Theoretical MW[d]	PHI-BLAST annotation[e]	EVpedia hit (E-value)[f]
71	Uncharacterized protein	Yes	18,113	No significant hit	No significant hit
72	Elongation factor 1-alpha	No	49,860	purR, tufA (*Staphylococcus aureus*) increased virulence in humans (Alkam et al., 2021)	*P. brasiliensis* (0.0) (Souza et al., 2019)
73	Uncharacterized protein	No	22,927	No significant hit	No significant hit
74	Uncharacterized protein	Yes	57,739	No significant hit	No significant hit
75	Similar to thimet oligopeptidase	Yes	85,569	No significant hit	*P. brasiliensis* (0.0)
76	Nep1, similar to necrosis-and ethylene-inducing protein 1	Yes	23,499	NLP2 of *Verticillium dahliae*, reduced virulence (Haddadi et al., 2016)	(Rutter & Innes, 2023)
77	Similar to amine oxidase	Yes	48,868	No significant hit	No significant hit
78	Similar to aspartyl aminopeptidase	No	74,178	Ape4 (*Cryptococcus neoformans*) reduced virulence in Mus musculus (Gontijo et al., 2017)	S. cerevisiae (1e-122) (Matos Baltazar et al., 2016)
79	Similar to amine oxidase	Yes	50,177	No significant hit	*M. xanthus* (4e-05)
80	Similar to FAD/FMN-containing isoamyl alcohol oxidase MreA	No	72,867	Zeb1 (*Fusarium graminearum*) unaffected pathogenicity (Lysoe et al., 2006)	Human (1e-04) (Bleackley et al., 2020)
81	DJ-1_PfpI domain-containing protein	Yes	28,520	OvrA (*Escherichia coli*) viurlence factor (Liu et al., 2020a)	No significant hit
82	Similar to endonu-clease/exonuclease/phosphatase family protein	Yes	33,899	No significant hit	No significant hit
84	Nucleoside diphosphate kinase	No	16,658	XC_2203 (*Xanthomonas campestris*) virulence factor (O'Connell et al., 2013)	*P. brasiliensis* (6e-89) (Vargas et al., 2015)
85	SurE domain-containing protein	No	46,429	No significant hit	No significant hit
87	Similar to starch binding domain containing protein	Yes	39,067	SGA1 (*Magnoporthe oryzae*) loss of pathogenicity on barley (Sauer et al., 2000)	*T. vaginalis* (6e-07)
88	Rhamnogalacturonan endolyase (EC 4.2.2.23)	Yes	69,044	No significant hit	No significant hit
89	Similar to actin	No	26,989	BcactA (*Botrytis cinerea*) virulence factor (Gupta et al., 2021)	S. cerevisiae (4e-153) (de Paula et al., 2019)
90	Predicted protein	Yes	14,838		
91	Similar to cellobiose dehydrogenase	Yes	82,678	BCIN_03g01540 (*Botrytis cinerea*) virulence factor (Zhang et al., 2020)	No significant hit
92	Glucanase	Yes	40,213	cbsA (*Xanthomonas oryzae*) virulence factor (Kumar et al., 2012)	No significant hit

(Continues)

TABLE 1 (Continued)

Rank[a]	Protein name[b]	Signal peptide[c]	Theoretical MW[d]	PHI-BLAST annotation[e]	EVpedia hit (E-value)[f]
93	Predicted protein	Yes	17,855	No significant hit	No significant hit
94	Similar to serine peptidase	Yes	60,220	No significant hit	*Drosophila melanogaster* (3e-32)
95	Transaldolase	No	53,539	talA (FTN_0781) *Francisella tularensis* reduced virulence on *Drosophila* (Rytter et al., 2021)	*P. brasiliensis* (1e-171) (Vargas et al., 2015)
96	Uncharacterized protein	No	22,809	No significant hit	No significant hit
97	Dipeptidyl-peptidase V	No	80,833	DPPIV (*Porphyromonas gingivalis*) virulence factor in mice (Kumagai et al., 2000)	*M. xanthus* (5e-93)
98	Similar to acetylxylan esterase 1	Yes	30,119	FAED1/FAEB1 (*Fusarium graminearum*) unaffected pathogenicity on wheat (Balcerzak et al., 2012)	No significant hit
99	Uncharacterized protein	No	102,630	No significant hit	*Pseudomonas syringae* pv. tomato (3e-45)
100	Similar to glutaminase	Yes	90,460	No significant hit	*P. brasiliensis* (0.0)
101	Similar to alpha-N-arabinofuranosidase	Yes	40,019	No significant hit	No significant hit
102	Carboxylic ester hydrolase	No	64,390	FGSG_03243 (*Fusarium graminearum*) reduced virulence (Zhang et al., 2016b)	Rat (2e-49)
103	Uncharacterized protein	Yes	46,414	No significant hit	No significant hit
104	Similar to beta-glucosidase	No	89,047	BcBGL3 (*Botrytis cinerea*) reduced virulence on tomato (Yao et al., 2016)	No significant hit
105	Predicted protein	Yes	12,577	No significant hit	No significant hit
106	Similar to alpha/beta hydrolase fold	Yes	35,647	STM14_RS07705 (*Salmonella enterica*) reduced virulence on lettuce (Montano et al., 2020)	*M. xanthus* (1e-21)
107	Beta-xylanase	Yes	34,947	xyn1 (*Ustilago maydis*) reduced virulence on maize (Moreno-Sanchez et al., 2021)	No significant hit
108	Similar to copper radical oxidase	No	97,941	GLX (*Fusarium verticillioides, F. oxysporum, F. graminaerum*) reduced virulence on wheat (Song et al., 2016)	Bovine (4e-16)
109	Uncharacterized protein	Yes	15,819	No significant hit	No significant hit
111	Similar to Pectin or pectate lyase-like protein Polysaccharide lyase family 1	Yes	88,123	No significant hit	No significant hit
112	Uncharacterized protein	No	65,367	BcBGL6 (*Botrytis cinerea*) reduced virulence on tomato (Zhang et al., 2020)	Bovine (2e-109)
113	Predicted protein	No	29,099	No significant hit	No significant hit
114	Histone H4	No	25,330	No significant hit	*P. basiliensis* (2e-66) (Bleackley et al., 2019)
115	Catalase	No	83,459	katG (*Acinetobacter nosocomialis*) increased virulence on *Galleria mellonella* (Sun et al., 2016)	*Acinetobacter baumannii* (0.0)

(Continues)

TABLE 1 (Continued)

Rank[a]	Protein name[b]	Signal peptide[c]	Theoretical MW[d]	PHI-BLAST annotation[e]	EVpedia hit (E-value)[f]
116	Alpha-mannosidase	No	126,414	No significant hit	*P. brasiliensis* (0.0)

[a]Order of identification.
[b]Protein name as suggested according to Mascot search results at Cambridge Centre for Proteomics; UniProt IDs and number of hits can be accessed from the supporting information.
[c]Signal peptide annotations were accessed via InterProScan and/or UniProt.
[d]Estimated sizes of mature peptides were estimated excluding signal peptides and potential glycosylation using amino acid sequence information from UniProt.
[e]Only significant hits were considered (E-values ≤ 1e-05); publications can be accessed from the Supporting information.
[f]E-values ≤ 1e-04 were considered based on protein sequence alignments; publications can be accessed from the Supporting information.

Enrichment analysis of gene ontology (GO) terms for molecular function revealed that glucosyl hydrolases were most significantly enriched, followed by peptidase activity and chitin binding (Figure 6). All three terms are expected to contribute to host-microbe interactions, although glycosyl hydrolases may specifically contribute to cell wall modifications and perhaps also to permeability of EVs within microbial or host cell walls. Catalase activity was also identified as an overrepresented GO term.

String analysis demonstrated a highly interconnected protein cluster involved in glucan hydrolase activities (Figure 7). Connecting with this cluster was a collection of proteins with diverse metabolic functions, including spermidine synthase, transaldolase, Glu dehydrogenase, catalases, nucleoside diphosphate kinase as well as actin, histone H4 and elongation factor 1-α (EF1A). Further connections occurred to a group of peptidases that included two α-mannosidases and an alkaline phosphatase. A separate group of six interconnected proteins were involved in chitin binding and/or metabolism, including a β-hexosaminidase. Polygalacturonase 1 and a pectate lyase involved in pectin degradation were also connected. Most of the proteins lacking a signal peptide were interconnected (63%, 22 of 35 proteins), whereas the minority of the conventionally secreted proteins (28%, 19 of

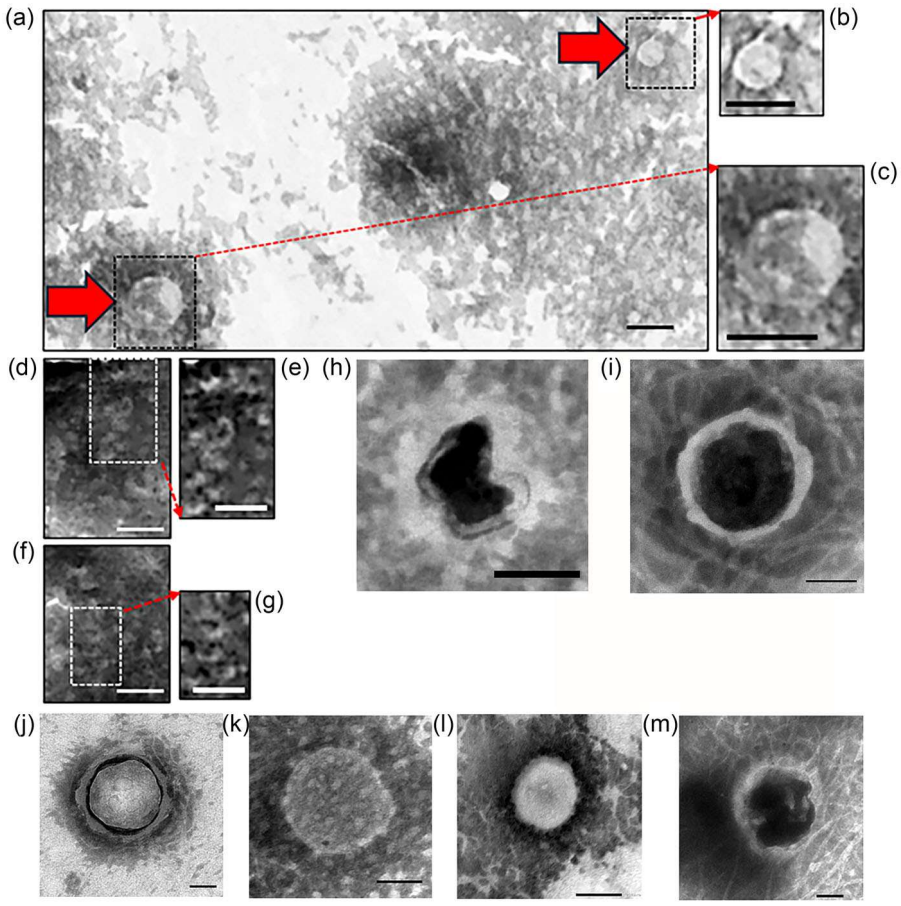

FIGURE 4 The extracellular vesicle (EV)-enriched fraction of *Leptosphaeria maculans* isolate v23.11.9 was prepared for electron microscopy using negative staining with phosphotungstic acid. No sectioning was done. (a) Two putative EVs (red arrows) lacking cup-shaped morphology, 80–120 nm in diameter, within one field of view; (b and c) magnifications. (d–g) Smaller cup-shaped EVs of ~50 nm diameter. (h) Larger cup-shaped EV ~130 nm in diameter. (i–m) Examples of larger EVs of >150 nm diameter; scale bars = 100 nm.

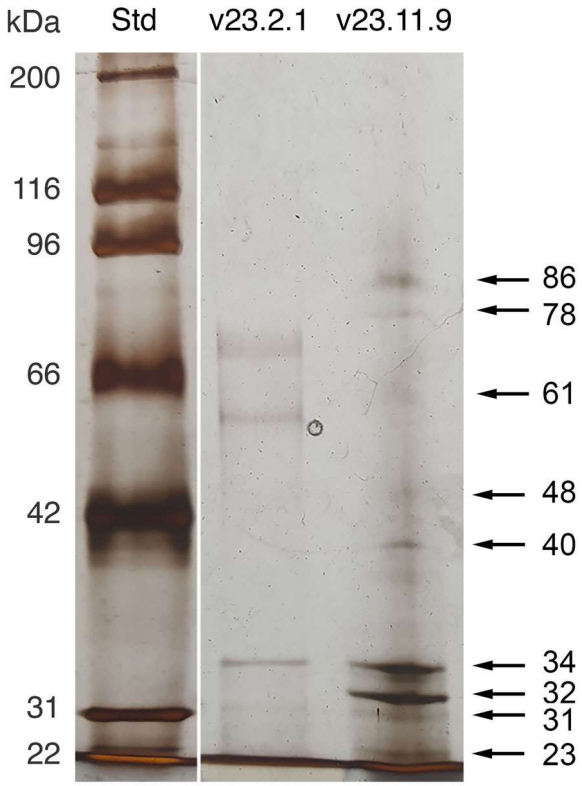

FIGURE 5 Silver-stained protein bands after SDS-PAGE of extracellular vesicle (EV)-enriched fractions of *Leptosphaeria maculans* isolates v23.2.1 and v23.11.9. Each EV-enriched sample contained 10 μg protein per lane. Molecular masses of the protein standard (Std) in kDa are indicated to the left and size estimates of stained bands from isolate v23.11.9 to the right of the gel.

69 proteins) had links, supportive of the fact that individually secreted proteins may not be connected. A total of 14 proteins were predicted or uncharacterised. This collective analysis suggests that the pelleted fraction collected was enriched in EVs, but we cannot exclude the possibility that some of the secreted proteins co-purified or contaminated the EVs that were obtained.

4 | DISCUSSION

This report provides the first glimpse at the role of EVs in interactions between *L. maculans* and its host *B. napus*. AFs could be extracted from infected cotyledons and leaves that were previously challenged with the fungal pathogen. It was easier to infiltrate and collect AFs from cotyledons than from leaves that were covered with a waxy cuticle. Initial experiments suggested that a concentration of 40 to 80 mg L^{-1} of Triton X-100 improved the yield of AFs from leaves. The total yield from cotyledons or leaves, however, was sufficient for particle analysis using NTA or silver staining or immunoblotting of proteins following SDS-PAGE. The NTA profile of AFs from *A. thaliana* leaves is not inconsistent with previous particle size estimates (Rutter & Innes, 2017; Zand Karimi et al., 2022). The maximum of the size distribution at 146 nm appears suggestive of P40-type vesicles although we also identified smaller vesicles perhaps reflective of exosome-like vesicles (Cai, Qiao et al., 2018). Unlike *A. thaliana*, *B. napus* apparently produces some larger EVs above 450 nm, but a more systematic analysis would be needed to make any conclusive claims in the absence of additional published data.

Silver staining consistently identified strong bands in the size range of ~40 kDa when analysing AFs from *B. napus*. Various cell wall modifying enzymes, including a β-1,3-glucanase, are similar in size (Brownfield & Howlett, 2001). RuBisCO was released into the apoplast solely after infection with *L. maculans* at 7 dpi. This stage of infection was previously identified as the onset of necrotic cell death in susceptible plants (Elliott et al., 2008); it is therefore suggested that RuBisCO release into the apoplast is facilitated by this transition to the necrotrophic stage of *L. maculans* colonisation (Stotz et al., 2023). Unexpectedly, however, RuBisCO was also observed in AFs during incompatible interactions with *L. maculans*, which may suggest that RuBisCO release into the apoplast may have other reasons, especially because *R* gene-mediated resistance was suggested to suppress host cell death (Becker et al., 2017; Haddadi et al., 2016). RuBisCO complexes of about 11 nm diameter were previously suggested to represent non-vesicular extracellular particles that pellet at 100,000 × *g* but remain in the supernatant at 40,000 × *g* (Rutter & Innes, 2020). The basis of RuBisCO release into the apoplast will therefore require more extensive investigation.

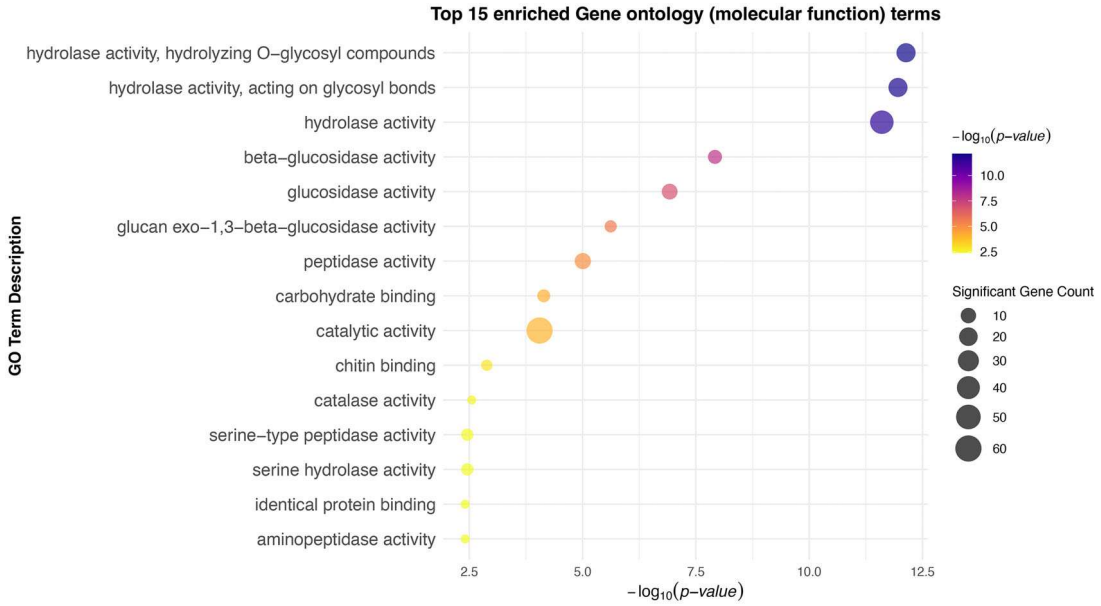

FIGURE 6 Enrichment analysis of gene ontology (GO) terms for molecular function. The 15 most enriched GO terms were displayed as a bubble plot, ranked according to their significance of enrichment using Fisher's exact test *P* values ($\log_{10}$ scale). Bubble sizes represent the counts of significant genes with colour indicating enrichment significance. Darker shades indicated lower *P* values and higher significance.

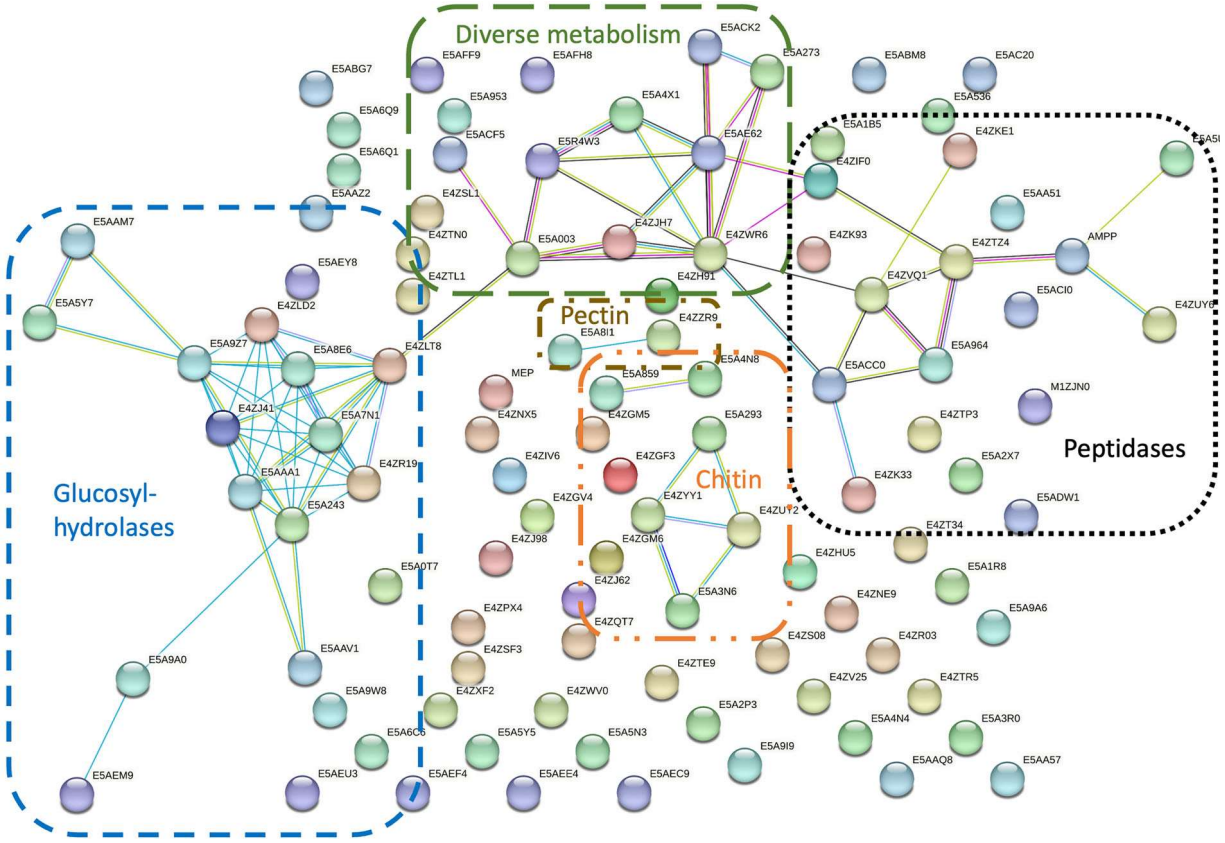

FIGURE 7 String analysis displaying networks of interacting proteins. Coloured nodes display query proteins and first shell of interactors. Edges are known interactions from curated databases (turquoise) or experimentally determined (pink); alternatively predicted interactions are shown from gene neighbourhoods (green) or gene cooccurrence (blue); otherwise, text mining (light green), co-expression (black) or protein homology (purple) are shown; *P*-value for protein-protein interaction (PPI) enrichment < 1.0 x e^{-16}. Identified clusters are indicated in blue (glucosyl hydrolases), black (peptidases), orange (chitin metabolism), brown (pectin metabolism) or green (diverse metabolism).

Infection with the *AvrLm1*-producing isolate v23.11.9 induced a chlorosis surrounding the necrotic lesion. This observation would suggest that *AvrLm1* enhances virulence, in agreement with published findings (Huang et al., 2010; Stotz et al., 2023). A corollary of this might be the enhanced RuBisCO release into the apoplast after host infection with an *AvrLm1*-producing pathogen isolate.

EVs isolated from culture filtrates of *L. maculans* had a similar NTA-based size distribution as previous reported data for certain phytopathogens (Costa et al., 2021; Hill & Solomon, 2020; Rizzo et al., 2021; Stotz et al., 2014), although the apparent NTA distributions of other fungi do vary (Bleackley et al., 2020; Bitencourt et al., 2018; de Paula et al., 2019; Reis et al., 2019). Moreover, the sizes and appearance of EVs visualised by TEM were reminiscent of previously visualised EVs (Costa et al., 2021; Hill & Solomon, 2020; Rayner et al., 2017), including previously documented cup-shaped morphologies that represent an artifact of dehydration during sample preparation (Kwon et al., 2021; Rutter et al., 2022). EV proteins from culture filtrates were separated by size and visualised by silver staining with bands ranging from ~20 to ~90 kDa, not dissimilar from a published report (Fernandes et al., 2023).

Proteomic analysis identified 35 proteins without a signal peptide, 14 of which were identified previously. In addition, over nine of the traditionally secreted proteins were reported in previous studies. Specifically, chitin deacetylases and glyoxal oxidase were noted in *Cryptococcus* species (Rizzo et al., 2021). Over 13 proteins, including a probable Xaa-Pro aminopeptidase, an FAD/FMN-containing isoamyl alcohol oxidase and EF1A were identified in EVs of *Aspergillus fumigatus* (Souza et al., 2019). In addition to other cell wall modification enzymes, α-mannosidases were previously identified in protoplasts of *A. fumigatus* (Rizzo et al., 2020); this is analogous to the role of matrix metalloproteinase and heparinase in modulation of the extracellular matrix (Al Halawani et al., 2022). Nucleotide diphosphate kinase, transaldolase, histone H4, glutamate dehydrogenase, phosphoglycerate mutase, endo-1,3(4)-β-glucanase, 1,3-β-glucanosyltransferase (BGL2) and β-hexosaminidase (HEX1) were reported in EVs of *Candida albicans* (Bleackley et al., 2019; Dawson et al., 2020; Martinez-Lopez et al., 2022; Vargas et al., 2015). *Trichoderma reesei* EVs were found to contain GH64 endo-1,3-β-glucanase and actin amongst others (de Paula et al., 2019). *F. graminearum* EVs were shown to contain a GPI-anchored β-1,3-endoglucanase (EglC), glutamate dehydrogenase and an extracellular glucoamylase amongst other proteins (Garcia-Ceron et al., 2021). *F. oxysporum* f. sp. *vasinfectum* EVs contain FAD-dependent oxidoreductases and a FAD-containing isoamyl alcohol oxidase (Bleackley et al., 2020). Aspartyl aminopeptidase and other proteins can be found in EVs of *Histoplasma capsulatum* (Matos Baltazar et al., 2016). Additional proteins are likely components of *L. maculans* EVs because they were identified using text annotations in Vesiclepedia (Chitti et al., 2024) and sequence searches in EVpedia, including glutaminase, amine oxidase, spermidine synthase, carboxypeptidase, alkaline phosphatase, carboxylesterase and catalase. Chitinase and effectors like Nep1 were also mentioned in a recent review of EVs from phytopathogenic fungi (Rutter & Innes, 2023). Although this may not be an exhaustive list, it clearly shows the amount of overlap between this and previous studies, thus validating the approach taken.

An enrichment analysis of GO terms for MF clearly implicated glucosyl hydrolases, peptidase activity, chitin binding and catalase activity as being important components of *L. maculans* EVs. This was confirmed by a network analysis using the STRING database, providing evidence for the interconnectedness of glucan catabolism, peptidase activities and other cellular (actin, histone H4, EF1A) or metabolic activities (catalases, nucleoside diphosphate kinase, spermidine synthase, transaldolase, glutamate dehydrogenase). Several interconnected proteins were part of chitin catabolism; two proteins involved in pectin catabolism were also connected. Collectively, this proteomics data provided the first evidence of the protein composition of EVs secreted by *L. maculans* into an axenic growth medium (Gamborg B5 with vitamins) that is also used for cultivation of plant cells. Cultivation of *L. maculans* in potato dextrose or V8 broth was not successful (Newbery et al., 2020; Stotz et al., 2023).

The *B. napus-L. maculans* pathosystem is a good model for studying interkingdom EV-mediated communication between host plants and apoplastic fungal pathogens, because EVs from both pathogen and host can be reliably harvested from AFs, in quantities sufficient for most downstream analytical work. This will include future applications for analysis of EV-mediated RNA interference (RNAi) using the same methods (Cai, Qiao et al., 2018). Although the role of EV protein cargoes is tantalising, it is the role of small RNAs (sRNAs) that has received much attention and conclusive evidence for being essential for interactions between fungal pathogens and host plants (Cai et al., 2023; Rutter & Innes, 2023). Distinguishing plant EV and fungal EV proteomes in mixed samples should not be a problem because of the comprehensive annotation of genomes/proteomes of both *B. napus* and *L. maculans* (Chalhoub et al., 2014; Rouxel et al., 2011). The preliminary characterisation of the *L. maculans* EV proteome will certainly help, and future efforts shall be directed to obtain similar information from uninoculated *B. napus* plants. It will, however, be challenging to collect large quantities of AFs from *B. napus* leaves because of their waxy cuticle, and cotyledons may therefore be used to improve the yield of AF collections. Experiments will certainly need to be scaled up for this purpose, but infected material can be accumulated simultaneously to compare the effect of different conditions on plant and pathogen EV composition. The proteins identified from *L. maculans* can be used as labels/markers for infection studies. It will be important to determine whether *Brassica* species contain tetraspanins and PEN1 to identify characteristic vesicle types (Huang et al., 2021). Further work will be needed to approach fungal EVs for such functionally comparative studies.

EVpedia proved to be an excellent resource for comparison (Kim et al., 2015). Despite this database being restricted to animals, animal pathogens and model organisms, many hits were identified, even in cases where no annotations were found using PHI-base. This finding raises the need for adding plant and plant microbe EV data to this database infrastructure, thus generating a

more comprehensive information for interorganismal EV cargo comparisons. This point will need to be raised with the research community working on plant-derived EVs (PDEVs).

5 AUTHOR CONTRIBUTIONS

Nathaniel Hearfield: Investigation (equal); writing—original draft (equal). **Dominik Brotherton**: Formal analysis (equal); visualization (equal); writing—review and editing (equal). **Zedi Gao**: Formal analysis (equal); methodology (equal); software (equal); writing—review and editing (equal). **Jameel Inal**: Methodology (equal); writing—review and editing (equal). **Henrik U. Stotz**: Conceptualization (equal); data curation (equal); formal analysis (equal); funding acquisition (equal); investigation (equal); methodology (equal); project administration (equal); supervision (equal); validation (equal); writing—review and editing (equal).

ACKNOWLEDGEMENTS

We are grateful to Dr Nicholas Larkan and Dr Hossein Borhan (Agriculture and Agri-Food Canada, Saskatoon, SK, Canada) for supplying seeds for the Topas-*LepR3* introgression line. We thank Kaan Sungur for contributing to EV analysis from uninfected plants and Dr Sufyan Akram for assistance with electron microscopy. We appreciate Lee Rixon's expertly advice on ultracentrifugation and chemiluminescent imaging. The British Society for Plant Pathology provided funding to NH. HUS was supported by the UK Biotechnology and Biological Sciences Research Council (BB/R019819/1).

CONFLICT OF INTEREST STATEMENT

The authors do not declare any conflicts of interest.

DATA AVAILABILITY STATEMENT

The data that support the findings of this study are available from the corresponding author upon reasonable request.

ORCID

Zedi Gao https://orcid.org/0009-0006-4777-8647
Jameel Inal https://orcid.org/0000-0002-7200-0363
Henrik U. Stotz https://orcid.org/0000-0003-2954-8566

REFERENCES

Al Halawani, A., Mithieux, S. M., Yeo, G. C., Hosseini-Beheshti, E., & Weiss, A. S. (2022). Extracellular vesicles: Interplay with the extracellular matrix and modulated cell responses. *International Journal of Molecular Sciences*, *23*, 3389.

Alkam, D., Jenjaroenpun, P., Ramirez, A. M., Beenken, K. E., Spencer, H. J., & Smeltzer, M. S. (2021). The Increased Accumulation of Staphylococcus aureus Virulence Factors Is Maximized in a purR Mutant by the Increased Production of SarA and Decreased Production of Extracellular Proteases. *Infection and Immunity*, *89*. https://doi.org/10.1128/IAI.00718-20

An, Q., Ehlers, K., Kogel, K. H., van Bel, A. J., & Huckelhoven, R. (2006). Multivesicular compartments proliferate in susceptible and resistant MLA12-barley leaves in response to infection by the biotrophic powdery mildew fungus. *New Phytologist*, *172*, 563–576.

Balesdent, M. H., Attard, A., Ansan-Melayah, D., Delourme, R., Renard, M., & Rouxel, T. (2001). Genetic control and host range of avirulence toward *Brassica napus* cultivars Quinta and Jet Neuf in *Leptosphaeria maculans*. *Phytopathology*, *91*, 70–76.

Baek, J. M., Howell, C. R., & Kenerley, C. M. (1999). The role of an extracellular chitinase from Trichoderma virens Gv29-8 in the biocontrol of Rhizoctonia solani. *Current Genetics*, *35*, 41–50. https://doi.org/10.1007/s002940050431

Balcerzak, M., Harris, L. J., Subramaniam, R., & Ouellet, T. (2012). The feruloyl esterase gene family of Fusarium graminearum is differentially regulated by aromatic compounds and hosts. *Fungal Biol*, *116*, 478–488. https://doi.org/10.1016/j.funbio.2012.01.007

Becker, M. G., Zhang, X., Walker, P. L., Wan, J. C., Millar, J. L., Khan, D., Granger, M. J., Cavers, J. D., Chan, A. C., Fernando, D. W. G., & Belmonte, M. F. (2017). Transcriptome analysis of the Brassica napus-*Leptosphaeria maculans* pathosystem identifies receptor, signaling and structural genes underlying plant resistance. *Plant Journal*, *90*, 573–586.

Bitencourt, T. A., Rezende, C. P., Quaresemin, N. R., Moreno, P., Hatanaka, O., Rossi, A., Martinez-Rossi, N. M., & Almeida, F. (2018). Extracellular vesicles from the dermatophyte trichophyton interdigitale modulate macrophage and keratinocyte functions. *Frontiers in Immunology*, *9*, 2343.

Bleackley, M. R., Dawson, C. S., & Anderson, M. A. (2019). Fungal extracellular vesicles with a focus on proteomic analysis. *Proteomics*, *19*, e1800232.

Bleackley, M. R., Samuel, M., Garcia-Ceron, D., McKenna, J. A., Lowe, R. G. T., Pathan, M., Zhao, K., Ang, C. S., Mathivanan, S., & Anderson, M. A. (2020). Extracellular vesicles from the cotton pathogen *Fusarium oxysporum* f. sp. vasinfectum Induce a phytotoxic response in plants. *Frontiers in Plant Science*, *10*, 1610.

Brownfield, L., & Howlett, B. J. (2001). An abundant 39 kDa protein from *Brassica napus* (canola) is present in the apoplast of leaves infected by the blackleg fungus, *Leptosphaeria maculans*. *Australasian Plant Pathology*, *30*, 7–9.

Cai, Q., Halilovic, L., Shi, T., Chen, A., He, B., Wu, H., & Jin, H. (2023). Extracellular vesicles: Cross-organismal RNA trafficking in plants, microbes, and mammalian cells. *Extracellular Vesicles and Circulating Nucleic Acids*, *4*, 262–282.

Cai, Q., Qiao, L., Wang, M., He, B., Lin, F. M., Palmquist, J., Huang, S. D., & Jin, H. (2018). Plants send small RNAs in extracellular vesicles to fungal pathogen to silence virulence genes. *Science*, *360*, 1126–1129.

Cai, X., Huang, Y., Jiang, D., Fitt, B. D. L., & Yang, L. (2018). Evaluation of oilseed rape seed yield losses caused by Leptosphaeria biglobosa in central China. *European Journal of Plant Pathology*, *150*, 170–190.

Chalhoub, B., Denoeud, F., Liu, S., Parkin, I. A., Tang, H., Wang, X., Chiquet, J., Belcram, H., Tong, C., Samans, B., Corréa, M., Da Silva, C., Just, J., Falentin, C., Koh, C. S., Le Clainche, I., Bernard, M., Bento, P., Noel, B., … Wincker, P. (2014). Plant genetics. Early allopolyploid evolution in the post-Neolithic Brassica napus oilseed genome. *Science*, *345*, 950–953.

Chitti, S. V., Gummadi, S., Kang, T., Shahi, S., Marzan, A. L., Nedeva, C., Sanwlani, R., Bramich, K., Stewart, S., Petrovska, M., Sen, B., Ozkan, A., Akinfenwa, M., Fonseka, P., & Mathivanan, S. (2024). Vesiclepedia 2024: An extracellular vesicles and extracellular particles repository. *Nucleic Acids Research*, *52*, D1694–D1698.

Chang, A., Khemlani, A., Kang, H., & Proft, T. (2011). Functional analysis of Streptococcus pyogenes nuclease A (SpnA), a novel group A streptococcal virulence factor. *Molecular Microbiology*, *79*, 1629–1642. https://doi.org/10.1111/j.1365-2958.2011.07550.x

Collins, N. C., Thordal-Christensen, H., Lipka, V., Bau, S., Kombrink, E., Qiu, J.-L., Hückelhoven, R., Stein, M., Freialdenhoven, A., Somerville, S. C., & Schulze-Lefert, P. (2003). SNARE-protein-mediated disease resistance at the plant cell wall. *Nature*, *425*, 973–977.

Costa, J. H., Bazioli, J. M., Barbosa, L. D., Dos Santos Junior, P. L. T., Reis, F. C. G., Klimeck, T., Crnkovic, C. M., Berlinck, R. G. S., Sussulini, A., Rodrigues, M. L., & Fill, T. P. (2021). Phytotoxic tryptoquialanines produced in vivo by *Penicillium digitatum* are exported in extracellular vesicles. *MBio*, *12*, e03393–20.

Dawson, C. S., Garcia-Ceron, D., Rajapaksha, H., Faou, P., Bleackley, M. R., & Anderson, M. A. (2020). Protein markers for *Candida albicans* EVs include claudin-like Sur7 family proteins. *Journal of Extracellular Vesicles*, *9*, 1750810.

Dalia, A. B., Standish, A. J., & Weiser, J. N. (2010). Three surface exoglycosidases from Streptococcus pneumoniae, NanA, BgaA, and StrH, promote resistance to opsonophagocytic killing by human neutrophils. *Infection and Immunity*, *78*, 2108–2116. https://doi.org/10.1128/IAI.01125-09

de Paula, R. G., Antoniêto, A. C. C., Nogueira, K. M. V., Ribeiro, L. F. C., Rocha, M. C., Malavazi, I., Almeida, F., & Silva, R. N. (2019). Extracellular vesicles carry cellulases in the industrial fungus *Trichoderma reesei*. *Biotechnology for Biofuels*, *12*, 1–14.

Deng, Y. Z., & Naqvi, N. I. (2010). A vacuolar glucoamylase, Sga1, participates in glycogen autophagy for proper asexual differentiation in Magnaporthe oryzae. *Autophagy*, *6*, 455–461. https://doi.org/10.4161/auto.6.4.11736

Deng, S., Sun, W., Dong, L., Cui, G., & Deng, Y. Z. (2019). MoGT2 Is Essential for Morphogenesis and Pathogenicity of Magnaporthe oryzae. *mSphere.*, *4*. https://doi.org/10.1128/mSphere.00309-19

Dufresne, M., van der Lee, T., Ben M'barek, S., Xu, X., Zhang, X., Liu, T., Waalwijk, C., Zhang, W., Kema, G. H., & Daboussi, M. J. (2008). Transposon-tagging identifies novel pathogenicity genes in Fusarium graminearum. *Fungal Genetics and Biology*, *45*, 1552–1561. https://doi.org/10.1016/j.fgb.2008.09.004

Elliott, C. E., Harjono, & Howlett, B. J. (2008). Mutation of a gene in the fungus *Leptosphaeria maculans* allows increased frequency of penetration of stomatal apertures of *Arabidopsis thaliana*. *Molecular Plant*, *1*, 471–481.

Fernandes, L. B., D'Souza, J. S., Prasad, T. S. K., & Ghag, S. B. (2023). Isolation and characterization of extracellular vesicles from *Fusarium oxysporum* f. sp. cubense, a banana wilt pathogen. *Biochimica Biophysica Acta General Subjects*, *1867*, 130382.

Fu, H., Feng, J., Aboukhaddour, R., Cao, T., Hwang, S. F., & Strelkov, S. E. (2013). An exo-1,3-beta-glucanase GLU1 contributes to the virulence of the wheat tan spot pathogen Pyrenophora tritici-repentis. *Fungal Biol*, *117*, 673–681. https://doi.org/10.1016/j.funbio.2013.07.003

Gallagher, J. R., Kim, A. J., Gulati, N. M., & Harris, A. K. (2019). Negative-stain transmission electron microscopy of molecular complexes for image analysis by 2D class averaging. *Current Protocols Microbiology*, *54*, e90.

Garcia-Ceron, D., Lowe, R. G. T., McKenna, J. A., Brain, L. M., Dawson, C. S., Clark, B., Berkowitz, O., Faou, P., Whelan, J., Bleackley, M. R., & Anderson, M. A. (2021). Extracellular vesicles from *Fusarium graminearum* contain protein effectors expressed during infection of corn. *Journal of Fungi (Basel)*, *7*, 977.

Garfoot, A. L., Dearing, K. L., VanSchoiack, A. D., Wysocki, V. H., & Rappleye, C. A. (2017). Eng1 and Exg8 Are the Major beta-Glucanases Secreted by the Fungal Pathogen Histoplasma capsulatum. *Journal of Biological Chemistry*, *292*, 4801–4810. https://doi.org/10.1074/jbc.M116.762104

Geoghegan, I. A., & Gurr, S. J. (2016). Chitosan Mediates Germling Adhesion in Magnaporthe oryzae and Is Required for Surface Sensing and Germling Morphogenesis. *Plos Pathogens*, *12*, e1005703. https://doi.org/10.1371/journal.ppat.1005703

Gontijo, F. A., de Melo, A. T., Pascon, R. C., Fernandes, L., Paes, H. C., Alspaugh, J. A., & Vallim, M. A. (2017). The role of Aspartyl aminopeptidase (Ape4) in Cryptococcus neoformans virulence and authophagy. *PLoS ONE*, *12*, e0177461. https://doi.org/10.1371/journal.pone.0177461

Gupta, R., Anand, G., Pizarro, L., Laor, D., Kovetz, N., Sela, N., Yehuda, T., Gazit, E., & Bar, M. (2021). Cytokinin Inhibits Fungal Development and Virulence by Targeting the Cytoskeleton and Cellular Trafficking. *MBio*, *12*, e0306820. https://doi.org/10.1128/mBio.03068-20

Haddadi, P., Ma, L., Wang, H., & Borhan, M. H. (2016). Genome-wide transcriptomic analyses provide insights into the lifestyle transition and effector repertoire of *Leptosphaeria maculans* during the colonization of Brassica napus seedlings. *Molecular Plant Pathology*, *17*, 1196–1210.

He, B., Cai, Q., Qiao, L., Huang, C. Y., Wang, S., Miao, W., Ha, T., Wang, Y., & Jin, H. (2021). RNA-binding proteins contribute to small RNA loading in plant extracellular vesicles. *Nature Plants*, *7*, 342–352.

Heimesaat, M. M., Schmidt, A. M., Mousavi, S., Escher, U., Tegtmeyer, N., Wessler, S., Gadermaier, G., Briza, P., Hofreuter, D., Bereswill, S., & Backert, S. (2020). Peptidase PepP is a novel virulence factor of Campylobacter jejuni contributing to murine campylobacteriosis. *Gut Microbes*, *12*, 1770017. https://doi.org/10.1080/19490976.2020.1770017

Hill, E. H., & Solomon, P. S. (2020). Extracellular vesicles from the apoplastic fungal wheat pathogen *Zymoseptoria tritici*. *Fungal Biology and Biotechnology*, *7*, 13.

Huang, Y., Wang, S., Cai, Q., & Jin, H. (2021). Effective methods for isolation and purification of extracellular vesicles from plants. *Journal of Integrative Plant Biology*, *63*, 2020–2030.

Huang, Y. J., Balesdent, M. H., Li, Z. Q., Evans, N., Rouxel, T., & Fitt, B. D. L. (2010). Fitness cost of virulence differs between the *AvrLm1* and *AvrLm4* loci in *Leptosphaeria maculans* (phoma stem canker of oilseed rape). *European Journal of Plant Pathology*, *126*, 279–291.

Huang, Y. J., Toscano-Underwood, C., Fitt, B. D. L., Hu, X. J., & Hall, A. M. (2003). Effects of temperature on ascospore germination and penetration of oilseed rape (*Brassica napus*) leaves by A- or B-group *Leptosphaeria maculans* (phoma stem canker). *Plant Pathology*, *52*, 245–255.

Hwang, S. F., Strelkov, S. E., Peng, G., Ahmed, H., Zhou, Q., & Turnbull, G. (2016). Blackleg (*Leptosphaeria maculans*) severity and yield loss in canola in Alberta, Canada. *Plants*, *5*, 31.

Isshiki, A., Akimitsu, K., Yamamoto, M., & Yamamoto, H. (2001). Endopolygalacturonase is essential for citrus black rot caused by Alternaria citri but not brown spot caused by Alternaria alternata. *Molecular Plant-Microbe Interactions*, *14*, 749–757. https://doi.org/10.1094/MPMI.2001.14.6.749

Jeon, H. S., Jang, E., Kim, J., Kim, S. H., Lee, M. H., Nam, M. H., Tobimatsu, Y., & Park, O. K. (2023). Pathogen-induced autophagy regulates monolignol transport and lignin formation in plant immunity. *Autophagy*, *19*, 597–615.

Jiquel, A., Gay, E. J., Mas, J., George, P., Wagner, A., Fior, A., Faure, S., Balesdent, M. H., & Rouxel, T. (2022). "Late" effectors from *Leptosphaeria maculans* as tools for identifying novel sources of resistance in *Brassica napus*. *Plant Direct*, *6*, e435.

Kim, D. K., Lee, J., Kim, S. R., Choi, D. S., Yoon, Y. J., Kim, J. H., Go, G., Nhung, D., Hong, K., Jang, S. C., Kim, S. H., Park, K. S., Kim, O. Y., Park, H. T., Seo, J. H., Aikawa, E., Baj-Krzyworzeka, M., van Balkom, B. W., Belting, M., … Gho, Y. S. (2015). EVpedia: A community web portal for extracellular vesicles research. *Bioinformatics*, *31*, 933–939.

Kumar, S., Haque, A. S., Jha, G., Sonti, R. V., & Sankaranarayanan, R. (2012). Crystallization and preliminary crystallographic studies of CbsA, a secretory exoglucanase from Xanthomonas oryzae pv. oryzae. *Acta Crystallographica Section F Structural Biology and Crystallization Communications*, *68*, 1191–1194. https://doi.org/10.1107/S1744309112034197

Kumagai, Y., Konishi, K., Gomi, T., Yagishita, H., Yajima, A., & Yoshikawa, M. (2000). Enzymatic properties of dipeptidyl aminopeptidase IV produced by the periodontal pathogen Porphyromonas gingivalis and its participation in virulence. *Infection and Immunity*, *68*, 716–724. https://doi.org/10.1128/IAI.68.2.716-724.2000

Kwon, S., Rupp, O., Brachmann, A., Blum, C. F., Kraege, A., Goesmann, A., & Feldbrügge, M. (2021). mRNA inventory of extracellular vesicles from *Ustilago maydis*. *Journal of Fungi*, *7*, 562.

Laemmli, U. K. (1970). Cleavage of structural proteins during the assembly of the head of bacteriophage T4. *Nature*, *227*, 680–685.

Larkan, N. J., Lydiate, D. J., Parkin, I. A., Nelson, M. N., Epp, D. J., Cowling, W. A., Rimmer, S. R., & Borhan, M. H. (2013). The *Brassica napus* blackleg resistance gene *LepR3* encodes a receptor-like protein triggered by the *Leptosphaeria maculans* effector AVRLM1. *The New Phytologist*, *197*, 595–605.

Larkan, N. J., Yu, F., Lydiate, D. J., Rimmer, S. R., & Borhan, M. H. (2016). Single *R* gene introgression lines for accurate dissection of the *Brassica—Leptosphaeria* pathosystem. *Frontiers in Plant Science*, *7*, 1771.

Leuthner, B., Aichinger, C., Oehmen, E., Koopmann, E., Müller, O., Müller, P., Kahmann, R., Bölker, M., & Schreier, P. H. (2005). A H2O2-producing glyoxal oxidase is required for filamentous growth and pathogenicity in Ustilago maydis. *Molecular Genetics and Genomics*, *272*, 639–650. https://doi.org/10.1007/s00438-004-1085-6

Li, Y., Xu, W., Zhang, F., Zhong, S., Sun, Y., Huo, J., Zhu, J., & Wu, C. (2020). The Gut Microbiota-Produced Indole-3-Propionic Acid Confers the Antihyperlipidemic Effect of Mulberry-Derived 1-Deoxynojirimycin. *mSystems*, *5*. https://doi.org/10.1128/mSystems.00313-20

Li, Y., Zhang, L., Wang, D., Zhou, H., Ouyang, H., Ming, J., & Jin, C. (2008). Deletion of the msdS/AfmsdC gene induces abnormal polarity and septation in Aspergillus fumigatus. *Microbiology (N YReading)*, *154*, 1960–1972. https://doi.org/10.1099/mic.0.2008/017525-0

Lin, H., Fischbach, M. A., Liu, D. R., & Walsh, C. T. (2005). In vitro characterization of salmochelin and enterobactin trilactone hydrolases IroD, IroE, and Fes. *Journal of the American Chemical Society*, *127*, 11075–11084. https://doi.org/10.1021/ja0522027

Liu, B., Wang, J., Wang, L., Ding, P., Yang, P., & Yang, B. (2020a). Transcriptional Activator OvrA Encoded in O Island 19 Modulates Virulence Gene Expression in Enterohemorrhagic Escherichia coli O157:H7. *Journal of Infectious Diseases*, *221*, 820–829. https://doi.org/10.1093/infdis/jiz458

Liu, X., Xie, J., Fu, Y., Jiang, D., Chen, T., & Cheng, J. (2020b). The Subtilisin-Like Protease Bcser2 Affects the Sclerotial Formation, Conidiation and Virulence of Botrytis cinerea. *International Journal of Molecular Sciences*, *21*. https://doi.org/10.3390/ijms21020603

Lowe, R. G., McCorkelle, O., Bleackley, M., Collins, C., Faou, P., Mathivanan, S., & Anderson, M. (2015). Extracellular peptidases of the cereal pathogen Fusarium graminearum. *Frontiers in Plant Science*, *6*, 962. https://doi.org/10.3389/fpls.2015.00962

Lysoe, E., Klemsdal, S. S., Bone, K. R., Frandsen, R. J., Johansen, T., Thrane, U., & Giese, H. (2006). The PKS4 gene of Fusarium graminearum is essential for zearalenone production. *Applied and environmental microbiology*, *72*, 3924–3932. https://doi.org/10.1128/AEM.00963-05

Martinez-Lopez, R., Hernaez, M. L., Redondo, E., Calvo, G., Radau, S., Pardo, M., Gil, C., & Monteoliva, L. (2022). *Candida albicans* hyphal extracellular vesicles are different from yeast ones, carrying an active proteasome complex and showing a different role in host immune response. *Microbiology Spectrum*, *10*, e0069822.

Matos Baltazar, L., Nakayasu, E. S., Sobreira, T. J., Choi, H., Casadevall, A., Nimrichter, L., & Nosanchuk, J. D. (2016). Antibody binding alters the characteristics and contents of extracellular vesicles released by *Histoplasma capsulatum*. *mSphere*, *1*, e00085–15.

Ma, L., Liu, T., Zhang, K., Shi, H., Zhang, L., Zou, G., & Sharon, A. (2022). Botrytis cinerea Transcription Factor BcXyr1 Regulates (Hemi-)Cellulase Production and Fungal Virulence. *mSystems*, *7*, e0104222. https://doi.org/10.1128/msystems.01042-22

Miyara, I., Shafran, H., Kramer Haimovich, H., Rollins, J., Sherman, A., & Prusky, D. (2008). Multi-factor regulation of pectate lyase secretion by Colletotrichum gloeosporioides pathogenic on avocado fruits. *Molecular plant pathology*, *9*, 281–291. https://doi.org/10.1111/j.1364-3703.2007.00462.x

Montano, J., Rossidivito, G., Torreano, J., Porwollik, S., Sela Saldinger, S., McClelland, M., & Melotto, M. (2020). Salmonella enterica Serovar Typhimurium 14028s Genomic Regions Required for Colonization of Lettuce Leaves. *Frontiers in Microbiology*, *11*, 6. https://doi.org/10.3389/fmicb.2020.00006

Moreno-Sanchez, I., Pejenaute-Ochoa, M. D., Navarrete, B., Barrales, R. R., & Ibeas, J. I. (2021). Ustilago maydis Secreted Endo-Xylanases Are Involved in Fungal Filamentation and Proliferation on and Inside Plants. *J Fungi (Basel)* 7. https://doi.org/10.3390/jof7121081

Newbery, F., Ritchie, F., Gladders, P., Fitt, B. D., & Shaw, M. W. (2020). Inter-individual genetic variation in the temperature response of Leptosphaeria species pathogenic on oilseed rape. *Plant Pathology*, *69*, 1469–1481.

O'Connell, A., An, S. Q., McCarthy, Y., Schulte, F., Niehaus, K., He, Y. Q., Tang, J. L., Ryan, R. P., & Dow, J. M. (2013). Proteomics analysis of the regulatory role of Rpf/DSF cell-to-cell signaling system in the virulence of Xanthomonas campestris. *Molecular Plant-Microbe Interactions*, *26*, 1131–1137. https://doi.org/10.1094/MPMI-05-13-0155-R

Pinedo, M., de la Canal, L., & de Marcos Lousa, C. (2021). A call for Rigor and standardization in plant extracellular vesicle research. *Journal of Extracellular Vesicles*, *10*, e12048.

Rayner, S., Bruhn, S., Vallhov, H., Andersson, A., Billmyre, R. B., & Scheynius, A. (2017). Identification of small RNAs in extracellular vesicles from the commensal yeast *Malassezia sympodialis*. *Scientific Reports*, *7*, 39742.

Reis, F. C. G., Borges, B. S., Jozefowicz, L. J., Sena, B. A. G., Garcia, A. W. A., Medeiros, L. C., Martins, S. T., Honorato, L., Schrank, A., Vainstein, M. H., Kmetzsch, L., Nimrichter, L., Alves, L. R., Staats, C. C., & Rodrigues, M. L. (2019). A novel protocol for the isolation of fungal extracellular vesicles reveals the participation of a putative scramblase in polysaccharide export and capsule construction in *Cryptococcus gattii*. *mSphere*, *4*, e00080–19.

Rizzo, J., Chaze, T., Miranda, K., Roberson, R. W., Gorgette, O., Nimrichter, L., Matondo, M., Latgé, J. P., Beauvais, A., & Rodrigues, M. L. (2020). Characterization of extracellular vesicles produced by *Aspergillus fumigatus* protoplasts. *mSphere*, *5*, e00476–20.

Rizzo, J., Wong, S. S. W., Gazi, A. D., Moyrand, F., Chaze, T., Commere, P. H., Novault, S., Matondo, M., Péhau-Arnaudet, G., Reis, F. C. G., Vos, M., Alves, L. R., May, R. C., Nimrichter, L., Rodrigues, M. L., Aimanianda, V., & Janbon, G. (2021). Cryptococcus extracellular vesicles properties and their use as vaccine platforms. *Journal of Extracellular Vesicles*, *10*, e12129.

Rouxel, T., Grandaubert, J., Hane, J. K., Hoede, C., van de Wouw, A. P., Couloux, A., Dominguez, V., Anthouard, V., Bally, P., Bourras, S., Cozijnsen, A. J., Ciuffetti, L. M., Degrave, A., Dilmaghani, A., Duret, L., Fudal, I., Goodwin, S. B., Gout, L., Glaser, N., … Howlett, B. J. (2011). Effector diversification within compartments of the *Leptosphaeria maculans* genome affected by repeat-induced point mutations. *Nature Communications*, *2*, 202.

Rouxel, T., Penaud, A., Pinochet, X., Brun, H., Gout, L., Delourme, R., Schmit, J., & Balesdent, M.-H. (2003). A 10-year survey of populations of *Leptosphaeria maculans* in France indicates a rapid adaptation towards the *Rlm1* resistance gene of oilseed rape. *European Journal of Plant Pathology*, *109*, 871–881.

Rose, J. K., Ham, K. S., Darvill, A. G., & Albersheim, P. (2002). Molecular cloning and characterization of glucanase inhibitor proteins: coevolution of a counterdefense mechanism by plant pathogens. *Plant Cell*, *14*, 1329–1345. https://doi.org/10.1105/tpc.002253

Rutter, B. D., Chu, T. T., Dallery, J. F., Zajt, K. K., O'Connell, R. J., & Innes, R. W. (2022). The development of extracellular vesicle markers for the fungal phytopathogen *Colletotrichum higginsianum*. *Journal of Extracellular Vesicles*, *11*, e12216.

Rutter, B. D., & Innes, R. W. (2017). Extracellular vesicles isolated from the leaf apoplast carry stress-response proteins. *Plant Physiology*, *173*, 728–741.

Rutter, B. D., & Innes, R. W. (2020). Growing pains: Addressing the pitfalls of plant extracellular vesicle research. *New Phytolology*, *228*, 1505–1510.

Rutter, B. D., & Innes, R. W. (2023). Extracellular vesicles in phytopathogenic fungi. *Extracellular Vesicles and Circulating Nucleic Acids*, *4*, 90–106.

Ruhela, D., Kamthan, M., Saha, P., Majumdar, S. S., Datta, K., Abdin, M. Z., & Datta, A. (2015). In vivo role of Candida albicans beta-hexosaminidase (HEX1) in carbon scavenging. *Microbiologyopen*, *4*, 730–742. https://doi.org/10.1002/mbo3.274

Rytter, H., Jamet, A., Ziveri, J., Ramond, E., Coureuil, M., Lagouge-Roussey, P., Euphrasie, D., Tros, F., Goudin, N., Chhuon, C., Nemazanyy, I., de Moraes, F. E., Labate, C., Guerrera, I. C., & Charbit, A. (2021). The pentose phosphate pathway constitutes a major metabolic hub in pathogenic Francisella. *Plos Pathogens*, *17*, e1009326. https://doi.org/10.1371/journal.ppat.1009326

Sanz-Martin, J. M., Pacheco-Arjona, J. R., Bello-Rico, V., Vargas, W. A., Monod, M., Díaz-Mínguez, J. M., Thon, M. R., & Sukno, S. A. (2016). A highly conserved metalloprotease effector enhances virulence in the maize anthracnose fungus Colletotrichum graminicola. *Molecular plant pathology*, *17*, 1048–1062. https://doi.org/10.1111/mpp.12347

Sarthy, A. V., McGonigal, T., Coen, M., Frost, D. J., Meulbroek, J. A., & Goldman, R. C. (1997). Phenotype in Candida albicans of a disruption of the BGL2 gene encoding a 1,3-beta-glucosyltransferase. *Microbiology (N YReading)*, *143*(Pt 2), 367–376. https://doi.org/10.1099/00221287-143-2-367

Sauer, J., Sigurskjold, B. W., Christensen, U., Frandsen, T. P., Mirgorodskaya, E., Harrison, M., Roepstorff, P., & Svensson, B. (2000). Glucoamylase: structure/function relationships, and protein engineering. *Biochimica Et Biophysica Acta*, *1543*, 275–293. https://doi.org/10.1016/s0167-4838(00)00232-6

Schouten, A., Tenberge, K. B., Vermeer, J., Stewart, J., Wagemakers, L., Williamson, B., & van Kan, J. A. (2002). Functional analysis of an extracellular catalase of Botrytis cinerea. *Molecular plant pathology*, *3*, 227–238. https://doi.org/10.1046/j.1364-3703.2002.00114.x

Souza, J. A. M., Baltazar, L. M., Carregal, V. M., Gouveia-Eufrasio, L., de Oliveira, A. G., Dias, W. G., Campos Rocha, M., Rocha de Miranda, K., Malavazi, I., Santos, D. A., Frézard, F. J. G., de Souza, D. D. G., Teixeira, M. M., & Soriani, F. M. (2019). Characterization of *Aspergillus fumigatus* extracellular vesicles and their effects on macrophages and neutrophils functions. *Frontiers in Microbiology*, *10*, 2008.

Song, X. S., Xing, S., Li, H. P., Zhang, J. B., Qu, B., Jiang, J. H., Fan, C., Yang, P., Liu, J. L., Hu, Z. Q., Xue, S., & Liao, Y. C. (2016). An antibody that confers plant disease resistance targets a membrane-bound glyoxal oxidase in Fusarium. *New Phytol.*, *210*, 997–1010. https://doi.org/10.1111/nph.13806

Stotz, H. U., Brotherton, D., & Inal, J. (2022). Communication is key: Extracellular vesicles as mediators of infection and defence during host-microbe interactions in animals and plants. *Fems Microbiology Review*, *46*, fuab044.

Stotz, H. U., Mitrousia, G. K., de Wit, P. J., & Fitt, B. D. L. (2014). Effector-triggered defence against apoplastic fungal pathogens. *Trends in Plant Science*, *19*, 491–500.

Stotz, H. U., Muthayil Ali, A., Robado de Lope, L., Rafi, M. S., Mitrousia, G. K., Huang, Y.-J., & Fitt, B. D. L. (2023). *Leptosphaeria maculans* isolates with variations in *AvrLm1* and *AvrLm4* effector genes induce differences in defence responses but not in resistance phenotypes in cultivars carrying the *Rlm7* gene. *Pest Managment Science*, *80*, 2435–2442.

Sun, D., Crowell, S. A., Harding, C. M., De Silva, P. M., Harrison, A., Fernando, D. M., Mason, K. M., Santana, E., Loewen, P. C., Kumar, A., & Liu, Y. (2016). KatG and KatE confer Acinetobacter resistance to hydrogen peroxide but sensitize bacteria to killing by phagocytic respiratory burst. *Life Sciences*, *148*, 31–40. https://doi.org/10.1016/j.lfs.2016.02.015

Switzer, R. C. 3rd, Merril, C. R., & Shifrin, S. (1979). A highly sensitive silver stain for detecting proteins and peptides in polyacrylamide gels. *Analytical Biochemistry*, *98*, 231–237.

Szklarczyk, D., Kirsch, R., Koutrouli, M., Nastou, K., Mehryary, F., Hachilif, R., Gable, A. L., Fang, T., Doncheva, N. T., Pyysalo, S., Bork, P., Jensen, L. J., & von Mering, C. (2023). The STRING database in 2023: Protein–protein association networks and functional enrichment analyses for any sequenced genome of interest. *Nucleic Acids Research*, *51*, D638–D646.

Tang, G., Xia, H., Liang, J., Ma, Z., & Liu, W. (2021). Spermidine Is Critical for Growth, Development, Environmental Adaptation, and Virulence in Fusarium graminearum. *Frontiers in Microbiology*, *12*, 765398. https://doi.org/10.3389/fmicb.2021.765398

Thery, C., Witwer, K. W., Aikawa, E., Alcaraz, M. J., Anderson, J. D., Andriantsitohaina, R., Antoniou, A., Arab, T., Archer, F., Atkin-Smith, G. K., Ayre, D. C., Bach, J. M., Bachurski, D., Baharvand, H., Balaj, L., Baldacchino, S., Bauer, N. N., Baxter, A. A., Bebawy, M., … Zuba-Surma, E. K. (2018). Minimal information for studies of extracellular vesicles 2018 (MISEV2018): A position statement of the International Society for Extracellular Vesicles and update of the MISEV2014 guidelines. *Journal of Extracellular Vesicles*, *7*, 1535750.

Tong, X., Wang, Y., Yang, P., Wang, C., & Kang, L. (2020). Tryptamine accumulation caused by deletion of MrMao-1 in Metarhizium genome significantly enhances insecticidal virulence. *Plos Genetics*, *16*, e1008675. https://doi.org/10.1371/journal.pgen.1008675

Urban, M., Cuzick, A., Seager, J., Wood, V., Rutherford, K., Venkatesh, S. Y., Sahu, J., Iyer, S. V., Khamari, L., De Silva, N., Martinez, M. C., Pedro, H., Yates, A. D., & Hammond-Kosack, K. E. (2022). PHI-base in 2022: A multi-species phenotype database for pathogen-host interactions. *Nucleic Acids Research*, *50*, D837–D847.

Vargas, G., Rocha, J. D., Oliveira, D. L., Albuquerque, P. C., Frases, S., Santos, S. S., Nosanchuk, J. D., Gomes, A. M., Medeiros, L. C., Miranda, K., Sobreira, T. J., Nakayasu, E. S., Arigi, E. A., Casadevall, A., Guimaraes, A. J., Rodrigues, M. L., Freire-de-Lima, C. G., Almeida, I. C., & Nimrichter, L. (2015). Compositional and immunobiological analyses of extracellular vesicles released by *Candida albicans*. *Cellular Microbiology*, *17*, 389–407.

Wang, C., Typas, M. A., & Butt, T. M. (2002). Detection and characterisation of prl virulent gene deficiencies in the insect pathogenic fungus Metarhizium anisopliae. *Fems Microbiology Letters*, *213*, 251–255. https://doi.org/10.1111/j.1574-6968.2002.tb11314.x

Wang, Z. Y., Soanes, D. M., Kershaw, M. J., & Talbot, N. J. (2007). Functional analysis of lipid metabolism in Magnaporthe grisea reveals a requirement for peroxisomal fatty acid beta-oxidation during appressorium-mediated plant infection. *Molecular Plant-Microbe Interactions*, *20*, 475–491. https://doi.org/10.1094/MPMI-20-5-0475

Welsh, J. A., Goberdhan, D. C. I., O'Driscoll, L., Buzas, E. I., Blenkiron, C., Bussolati, B., Cai, H., Di Vizio, D., Driedonks, T. A. P., Erdbrügger, U., Falcon-Perez, J. M., Fu, Q. L., Hill, A. F., Lenassi, M., Lim, S. K., Mahoney, M. G., Mohanty, S., Möller, A., Nieuwland, R., … Witwer, K. W. (2024). Minimal information for studies of extracellular vesicles (MISEV2023): From basic to advanced approaches. *Journal of Extracellular Vesicles*, *13*, e12404.

Wilson, L. M., Idnurm, A., & Howlett, B. J. (2002). Characterization of a gene (sp1) encoding a secreted protein from *Leptosphaeria maculans*, the blackleg pathogen of *Brassica napus*. *Molecular Plant Pathology*, *3*, 487–493.

Yao, G., Wu, R., Kan, Q., Gao, L., Liu, M., Yang, P., Du, J., Li, Z., & Qu, Y. (2016). Production of a high-efficiency cellulase complex via beta-glucosidase engineering in Penicillium oxalicum. *Biotechnology for Biofuels*, *9*, 78. https://doi.org/10.1186/s13068-016-0491-4

Yan, T., Zhou, X., Li, J., Li, G., Zhao, Y., Wang, H., Li, H., Nie, Y., & Li, Y. (2022). FoCupin1, a Cupin_1 domain-containing protein, is necessary for the virulence of Fusarium oxysporum f. sp. cubense tropical race 4. *Frontiers in Microbiology*, *13*, 1001540. https://doi.org/10.3389/fmicb.2022.1001540

Zand Karimi, H., Baldrich, P., Rutter, B. D., Borniego, L., Zajt, K. K., Meyers, B. C., & Innes, R. W. (2022). Arabidopsis apoplastic fluid contains sRNA- and circular RNA-protein complexes that are located outside extracellular vesicles. *Plant Cell*, *34*, 1863–1881.

Zheng, X., Koopmann, B., Ulber, B., & von Tiedemann, A. (2020). A global survey on diseases and pests in oilseed rape—Current challenges and innovative strategies of control. *Frontiers in Agronomy*, *2*, 590908.

Zhang, M. Z., Sun, C. H., Liu, Y., Feng, H. Q., Chang, H. W., Cao, S. N., Li, G. H., Yang, S., Hou, J., Zhu-Salzman, K., Zhang, H., & Qin, Q. M. (2020). Transcriptome analysis and functional validation reveal a novel gene, BcCGF1, that enhances fungal virulence by promoting infection-related development and host penetration. *Molecular plant pathology*, *21*, 834–853. https://doi.org/10.1111/mpp.12934

Zhang, L. B., Tang, L., Ying, S. H., & Feng, M. G. (2016a). Distinct roles of two cytoplasmic thioredoxin reductases (Trr1/2) in the redox system involving cysteine synthesis and host infection of Beauveria bassiana. *Applied Microbiology and Biotechnology*, *100*, 10363–10374. https://doi.org/10.1007/s00253-016-7688-0

SUPPORTING INFORMATION

Additional supporting information can be found online in the Supporting Information section at the end of this article.

How to cite this article: Hearfield, N., Brotherton, D., Gao, Z., Inal, J., & Stotz, H. U. (2025). Establishment of an experimental system to analyse extracellular vesicles during apoplastic fungal pathogenesis. *Journal of Extracellular Biology*, *4*, e70029. https://doi.org/10.1002/jex2.70029